U.S. DEPARTMENT OF THE INTERIOR
U.S. GEOLOGICAL SURVEY

MAPPING TOPOGRAPHIC FORM by DIGITAL IMAGE-PROCESSING in the SAN JOSE 1:100,000 SHEET, CALIFORNIA

by

Richard J. Pike[1], William Acevedo[2], and Patrick K. Showalter[3]

Open-File Report OF92-420

[1]Menlo Park, California 94025
[2]Moffett Field, California 94035
[3]Current address: ESRI Inc., Reston, Virginia 22090

CONTENTS

LIST OF FIGURES

LIST OF MAPS

• Maps 4-20 computed by authors from gridded contours of the San Jose 1:100,000-scale sheet (U.S.Geological Survey, 1978)

Mapping Topographic Form by Digital Image-Processing in the San Jose 1:100,000 Sheet, California

by

Richard J. Pike, William Acevedo, and Patrick K. Showalter

ABSTRACT

Topography that is sampled on a dense X,Y grid of terrain heights can be described and analyzed rapidly by the techniques of digital image-processing. This semi-automated approach to terrain representation was applied to continuous topography (as distinguished from discrete landforms) by creating 17 thematic maps, in color or in 255 gray tones, derived from elevations over a 4940-km^2 area in northern California.

The digital elevation model (DEM) of the 1:100,000-scale San Jose quadrangle is one of the first in a new medium-scale series created by the Geological Survey through the interpolation of contour maps by computer. The 2,000,000 terrain elevations, spaced two arc-seconds (typically 55 m) apart on a rectilinear grid, are more accurate than the heights in older DEMs although some artifacts remain from the interpolation routine and edge-matching of subquads.

Digitally sampled topography in the San Jose area was displayed qualitatively through computer graphics. Shaded-relief images, calculated for different values of Sun elevation and azimuth and plotted on a film recorder in visually continuous gray tones, create contrasting perspectives on the area. Computer shading not only shows landforms accurately and in their true complexity, but does so in single synoptic views that provide a broad regional context for geologic interpretation.

Topography in the San Jose quadrangle also was described quantitatively, by measuring attributes shown in prior work to be particularly diagnostic of surface form. Among the selected derivatives of elevation computed from the DEM by a new C-language software package and mapped on a color plotter are mean height, local relief, skewness of elevation, angles of slope and curvature, and frequency of slope reversal (a measure of landform spacing).

Digital maps of the six measures were combined statistically, by an automated procedure adapted from Landsat image analysis, to identify topographic types in the San Jose area. Occurrences of the five resulting types—roughlands (three categories), low plains, and plains-roughlands border—cluster spatially to form putative terrain units. The minimal correlation of most of these units with geology, however, suggests the need for experimenting with different measures of terrain form. Alternatively, topography within the small area covered by the San Jose quadrangle may be too homogeneous to warrant subdivision beyond eroding upland and alluvial plains.

INTRODUCTION

The San Jose 1:100,000-scale map sheet (see map 1) is part of the Southern San Francisco Bay Region Geologic Framework Project, a major study unit of the Geological Survey's National Geologic Mapping Program (for example, Wentworth and Blake, 1991). Geologic maps of the area at 1:100,000 scale are being compiled in a digital data base from existing sources (Fitzgibbon and others, 1991) and supplemented by new mapping in selected localities. Although directed largely at geology and geophysics in digital map format, a contributing element to the data base is topography. This report describes computer-compiled maps of terrain slope, shaded relief, and other measures of surface form that further support regional analysis in the San Jose study area.

The San Jose 1:100,000 map sheet is located in the central Coast Ranges of California, which consist of NW-trending alluvial valleys and geologically complex ranges of low mountains (U.S. Geological Survey, 1978). The four main physiographic elements of the San Jose sheet, from west to east, are the Santa Cruz Mountains, the Santa Clara Valley, the southern Diablo Range, and the San Joaquin Valley. The sheet extends from the eastern outskirts of Santa Cruz on Monterey Bay to Gustine in the San Joaquin Valley, and includes an area of high urban growth in the Santa Clara Valley at the southern end of San Francisco Bay. Most of Santa Clara County and parts of Stanislaus, Merced, Santa Cruz, and Alameda counties lie within the quadrangle.

The metric 1:100,000-scale topographic sheet (U.S. Geol. Survey, 1978) occupies the southwest quadrant of the AMS/USGS two-degree (1:250,000-scale) topographic sheet (U.S. Geol. Survey, 1969). The latter (map 1) serves as general location map for features named in this report; it is included here rather than the 1:100,000-scale map because it is more legible at publication size.

The geology of the area is described by Bailey (1966), Rogers (1966) (see map 2), Wagner and others (1990), and Wentworth and Blake (1991), and is summarized in Abrams (1992). Among major features are segments of the throughgoing San Andreas and Silver Creek-Calaveras faults and the epicenter of the 1989 Loma Prieta earthquake in the Santa Cruz Mountains (about 5 km southwest of the San Andreas Fault zone). Additional NW-striking faults that show evidence of Quaternary displacement are common in the western half of the sheet. Other important features include limestones and volcanics that host the largest mercury deposit in North America (New Almaden), the Diablo Mountain Range—developed on upper Mesozoic rocks of the Franciscan assemblage (and the site of a proposed reservoir to supplement the area's water supply), and extensive deposits of Quaternary alluvium in the Santa Clara and San Joaquin Valleys. Landslides are common in the steep terrain of both mountain ranges.

COMPUTER ANALYSIS OF TOPOGRAPHY

Information germane to many Earth-science problems and related applications, in the San Jose quadrangle and elsewhere, is encoded in topographic form. Recent advances in computer technology, particularly developments in digital cartography, have simplified the extraction of much of this information for geologic inference. The large, dense arrays of X,Y-gridded terrain heights, or digital elevation models (DEMs; fig. 1), that are are created by

the Geological Survey's National Mapping Division and other agencies (U.S. Geological Survey, 1990) can effectively capture topographic form. These data may be analyzed by specialized software and the resulting maps of DEM derivatives printed on large-format output devices (Brabb, 1987; Pike and others, 1987). The maps range from simple three-point calculations of terrain slope and aspect, through such complex derivatives as slope curvature and shaded relief, to multivariate statistical models of topographic form and their spatial variation (Pike and Acevedo, 1988; Dikau and others, 1991; Reichenbach and others, 1992).

Perceptual and parametric representation The information content of continuous topography that is sampled by a DEM can be communicated visually or analytically, and we have included examples of both methods in this report. Digital terrain is expressed *perceptually*, in qualitative terms, by shaded-relief images and other means of visualization provided by computer graphics (Kennie and McLaren, 1988; Thelin and Pike, 1991; Simpson and Anders, 1992). The computer-shaded San Jose DEM not only depicts landforms accurately and in their true complexity, at the resolution of the data—close to that of 1:24,000-scale topographic maps, but does so in single synoptic views (maps 13 and 14) that provide a broad regional context for analysis and interpretation of the area's geology, natural hazards, and land use.

Digitally sampled terrain also is described *parametrically*, by measuring and mapping different attributes of surface form. Among the most effective of these are the first three statistical moments (central tendency, dispersion, and skewness) of elevation, slope, and curvature (Tobler, 1969; Evans, 1972). Values of slope angle, aspect, and other measures calculated at each locale constitute *geometric signatures*, multivariate fingerprints that characterize topographic form (Pike, 1988a and b). Several derivatives of elevation have been mapped for this report (maps 5-12, 15-19). Combining such individual maps statistically by computer has enabled us to recognize different topographic types in the San Jose quadrangle. Where occurrences of the types cluster spatially, possible terrain units may be defined (map 20; Hammond, 1964; Pike, 1972).

Discrete and continuous sampling The techniques of computer cartography can represent topography in two distinct ways, depending on whether the sample design used to analyze a DEM is discrete or continuous (Mark, 1978). Each approach has different advantages for topographic analysis. Although maps 4-20 were computed from continuous sampling, we describe discrete sampling in some detail to highlight the chief differences between the two.

Discrete (or *specific* in the terminology of Evans, 1972) sample units are irregularly shaped cells of variable size that outline individual landforms, such as watersheds, landslides, volcanoes, sand dunes, drumlins, and impact craters (Pike, 1974). Measurements—of width, height, area, volume, and planimetric shape—made on these landform units relate directly to the operation of geomorphic processes. For this reason, such discrete sample units as watersheds often are referred to as process-response units.

Discrete terrain units may be defined from DEMs for some types of landforms by *feature extraction*, a continuous-to-discrete transformation developed as a technique of image-processing (Jensen, 1986). The most important

example of this transformation is an automated procedure that generates an integrated system of fluvial watersheds from a DEM (for example, Band, 1986; Jenson and Domingue, 1988). We have partly implemented the approach in this report by using slope reversal to identify (non-integrated) ridges and drainageways on which to calculate such descriptors of topography as slope curvature.

A less complete continuous-to-discrete transformation, the triangulated irregular network (TIN), converts a DEM into nonoverlapping triangles that approximate hillslope terrain facets, referred to as *surface-specific* units (Peucker and others, 1978). The automated TIN procedure, which is still maturing computationally, has not been explored further in this report, although we have experimented with it in areas adjacent to the San Jose quadrangle (Pike and others, 1987).

Where discrete unit-cells are not (as here) formally defined, topographic form may be mapped by continuous sampling. Unit cells for continuous (or *general*, in the terminology of Evans, 1972) sampling of a DEM typically are rectangles of a constant and (usually) arbitrary size, called windows or subgrids. For example, slope angle may be computed over a large area by moving a 3x3 subgrid of elevations one pixel at a time (maps 10, 11). This approach is well established from the analysis of multispectral images obtained from spacecraft (Jensen, 1986). Although lacking the direct process-response linkage built into discrete units, continuous sampling nonetheless reflects geomorphic process and additionally has advantages of speed, simplicity, and computational efficiency. The continuous mode—used to compute slope, relief, and other variables for this report—allows a large area to be analyzed rapidly from a DEM by writing uncomplicated software or by adapting existing image-processing algorithms. The discrete-unit approach is more difficult to implement computationally.

THE DIGITAL ELEVATION MODEL

Our experimental observations, a DEM of terrain heights arrayed in a rectangular grid, were created by the Survey's National Mapping Division (NMD) (U.S. Geological Survey, 1990) through semi-automated digitizing of contour lines on the 1:100,000-scale San Jose topographic sheet (fig. 1). Map 3, the digital line graph (DLG), shows contours of the 1:100,000-scale topographic map replotted at a smaller scale. NMD interpolated contour elevations to a grid at two arc-seconds resolution (about 55 m on the ground, depending on latitude), to yield a dense 1122 X 1802 array of about 2,000,000 heights for the 89 X 55.5-km quadrangle. Figure 1 illustrates this process for an earlier data set created for the entire United States from 1:250,000-scale maps (Mays, 1966; Thelin and Pike, 1991).

Despite artifacts of the gridding (fig. 4) and subquad-paneling procedures and the absence of such refinements as water-body outlines, we judge the new 1:100,000-scale data as presently published to be adequate for the experimental maps shown here (Acevedo, 1991). The new map's 50-meter elevation contours (and supplementary 10-m contours and spot heights) appear to portray the topography of the 1978 San Jose 1:100,000 sheet (map 3) more accurately and in slightly greater detail than the 200-foot contours of the older 1:250,000-scale map (map 1)—especially in areas of low relief. We did not compare the two quantitatively. The improvement in quality of the two-arc-second DEM over that of

the three-arc-second DEM for the same area (Mays, 1966) is clearly evident in the visual comparison of shaded-relief images computed for both sets of data by Acevedo (1991, fig. 1).

DIGITAL IMAGE-PROCESSING

The method used to compute maps 4-20 is related to the broader fields of computer graphics and machine vision (Kennie and McLaren, 1988). Digital image-processing includes spatial filtering, contrast-enhancement, and the many other operations first brought together and developed to manipulate Ranger, Mariner, Landsat, and other images that are reassembled from spacecraft telemetry in a scan-line (raster) arrangement of square-grid picture elements (pixels). These computer procedures were transferred to landform analysis from remote-sensing applications (for example Swain and Davis, 1978; Jensen, 1986), simply by substituting terrain heights or sea-floor depths for the customary values of measured reflectance acquired by satellites.

In uniform X,Y-gridded arrays, the computer keeps track of locations implicitly rather than having to specify them individually. This economy enables image-processing algorithms to rapidly map digital elevations and their derivatives over large areas (Batson and others, 1975; Burrough, 1986). Digital maps such as those shown here for the San Jose 1:100,000 DEM can then be compared and combined with other types of gridded data (for example, Colleau and Lenôtre, 1991), often by means of a raster-based geographic information system (GIS).

Elevation derivatives are mapped from a DEM in four steps: (1) Select a sample design, such as a local sub-grid (or window) of terrain heights—for example a 3X3 elevation matrix used to compute point-slope angle (fig. 2). One window size may not suit all measures. (2) For each measure, move the sub-grid systematically through the DEM, commonly one grid point at a time, computing a value over the entire window but assigning it to the central location (fig. 3), until the entire array is characterized. (3) Prepare hardcopy by scaling the resulting range of values into suitable intervals (bins) after studying a histogram of the values and then assigning a color or gray value to each interval. (4) Print the map on a color or monochrome plotter or other output device.

We made the maps by processing the DEM through analytical software of our own design, installed on a Silicon Graphics 4D/85GT 32-bit Unix workstation. The software, provisionally named the Terrain Analysis Package (TAP) computes digital maps of slope angle and other variables. It is outlined in Table 1. This C-language package has been used to process an even larger DEM of Italy (Reichenbach and others, 1992); it is not yet complete. For this report, the maps that required a moving sample space (a 37 X 37-pixel window, roughly a 2 X 2 km rectangle) each required about an hour of processing time, the others less than ten minutes. The software used to divide the area into topographic types is described below in the discussion of map 20.

The 20 maps in this report, numbered separately from text figures, were reduced to publication size (about 1:375,000 scale) from the originals (1:250,000 scale) by xerography. The four continuous-tone black-and-white images were printed from negatives made on a film recorder (an Optronics device used here); the 13 color maps were produced on an electrostatic plotter (a Calcomp machine

used here). Maps 1-3 are of hypsography or geology. Maps 4-20 display the DEM in altitude-tint format, plus the following derivatives: shaded relief; elevation maximum (envelope), minimum (subenvelope), and mean (central tendency); local relief (elevation dispersion); the elevation-relief ratio (elevation skewness); slope aspect (azimuth); slope angle; slope reversals (ridge and drainage net); frequency of slope reversal (texture); cross-ridge and cross-valley curvature at slope reversals; mean curvature; and topographic types computed from six of the above maps.

The ranges assigned to units in many of the following maps are not the usual round-numbered intervals. The unconventional bins result from rescaling the 0-255 range (required to compute the data through image-processing software) back to the original units of measurement (Jensen, 1986). These maps also are preliminary in several respects; for example, even such large water bodies as the San Luis, Calaveras, and Anderson reservoirs (map 1) are not shown.

SINGLE-FACTOR MAPS

Elevation (map 4) An elevation-tint map is a common method for generalizing the hypsography of an area. This detailed display of topography in the San Jose quadrangle was made by dividing the altitude range of the entire DEM (fig. 4) into ten 128-m bins (except for the first two and the last bins: 0-25 m, 26-128 m, and 1026-1308 m, respectively) and printing the resulting distributions in color at one-pixel (about 0.2 mm at 1:375,000 scale) resolution. The elevation ranges from zero in southern San Francisco Bay to 1308 m at Copernicus Peak on the Mt. Hamilton ridge in the Diablo Range. We experimented with transforming elevation to logarithms or to square roots (maps not shown) in an attempt to reduce the strong skewness of the elevation histogram (fig. 4), but found that such changes did not improve on the ability of the raw DEM to express the topographic morphology of the area. Valleys marking the traces of throughgoing faults, for example, still are best seen on this arithmetically plotted map of elevation.

Mean Elevation (map 5) This map further generalizes map 4. The DEM is averaged on a 2x2-km window moved through the DEM one pixel at a time and contoured at the same intervals as map 4. Map 5 shows the first statistical moment of terrain height (central tendency, in this case over a 37 x 37-pixel unit cell). It is unencumbered by the morphologic detail contained in map 4, shows only overall trends, and thus may be especially suited for applications that require visual or superposed comparison with other types of generalized data (for example, depth-to-bedrock, gravity and magnetics).

Maximum Elevation (map 6) For addressing certain objectives in landform analysis, typically requiring estimates of summit accordance, elevation also may be generalized by mapping extreme values rather than central tendency (Pannekoek, 1967; Colleau and Lenôtre, 1991). Map 6 was made by assigning the highest elevation in a 2X2-km window to the central pixel in that window, moving the window one grid point at a time through the DEM, and mapping the result in the same height intervals used for maps 4 and 5. The distinctly blocky appearance of this and the two following images (unlike maps 4 and 5) results from the window-mapping of isolated extreme values of elevation. A somewhat

different version of this type of map, constructed manually from ridge-crest heights shown by contours, is referred to by geomorphologists as an *envelope map* (Stearns, 1967). It is helpful in reconstructing and visualizing pre-dissection upland surfaces. Strictly speaking, map 6 map is a pseudo-envelope map.

Minimum Elevation (map 7) In this complement of map 6, the lowest elevation in a 37 x 37-pixel window is similarly mapped—using the same elevation intervals and colors. A somewhat different version of this map, compiled manually from drainageway elevations on contour maps, is termed a *subenvelope map* by geomorphologists (Stearns, 1967). It is helpful in generalizing the surface toward which regional dissection is proceeding. This pseudo-subenvelope map differs considerably from map 6, a result of the substantial changes in relief pattern within short distances in this area (compare, for example, the highland centered on Mt. Hamilton). The contrast between maps 6 and 7 also suggest that the 2x2-km window was an apt choice of a sample size to record and generalize the gross features that are typical of this area's topography (1 km or 5 km windows would have resulted in less contrasting maps).

Local Relief (map 8) Local, or relative relief, is the difference between highest and lowest elevation in a specified unit-cell (Smith, 1935; Drummond and Dennis, 1968). Computed by subtracting the pseudo-subenvelope (map 7) from its complement (map 6), this map of the San Jose 1:100,000 sheet on a 2x2 km window gives a good overall picture of elevation contrast and terrain roughness. It is equivalent to elevation dispersion (in this case, the range), the second statistical moment of terrain height (Evans, 1972). (Alternatively, standard deviation could have been computed.) The color convention remains the same as that for the previous maps. This map surpasses that of raw hypsography in highlighting upland valleys in the Diablo Range. It further reveals that terrain between Black Mountain and Poverty Ridge, southeast of the Calaveras Reservoir (see map 1), is by far the largest area of high local relief (about 800 m) in the quadrangle.

Elevation-Relief Ratio (map 9) This measure is mathematically identical (Pike and Wilson, 1971) to the hypsometric integral (Strahler, 1952) and approximately equivalent to elevation skewness—the third statistical moment of terrain height (fig. 5). The elevation-relief ratio, **E**, is computed rapidly by the simple expression

$$\mathbf{E} = (H_{mean}-H_{min}) / (H_{max}-H_{min}) \qquad (1)$$

(Wood and Snell, 1960) where mean, maximum, and minimum values of terrain height H all are determined within a window moved through the DEM in one-pixel increments. Values of **E**, mapped here in four bins, range from near zero (theoretically a low plain with one small hummock) to near 1.0 (a plateau with one narrow incision). Because the parameter loses its descriptive capacity in smooth topography, areas of the map with less than about 50 m of local relief are masked out (here manually, although it could be done in the computer using the data in map 8). At the chosen window size, 2x2 km, large areas in the San Jose sheet rarely exceed **E** values of 0.65 (massive, often relatively flat-topped ridges; for

example, Palassou and Blue Ridges) or fall below values of 0.20 (inland or plains-neighboring valleys; for example, Isabel and San Antonio Valleys).

Slope Angle—color (map 10) Slope is the first vertical derivative of elevation (Tobler, 1969). Commonly considered the single measure that best describes topographic form (Wood and Snell, 1960; Evans, 1972), slope angle here is calculated on a small, 3X3-pixel, window (fig. 2) moved one pixel at a time, and the resulting value assigned to the central pixel. The range of slopes, from zero to at least 45 degrees (fig. 6), is parsed into eight five-degree bins and one for slopes over 40 degrees. Erroneous high values at the map margin, called edge effects, exceed 45 degrees. In map 10, bins two and three (five to 15 degrees) were combined inadvertently (an oversight not corrected for this report). The color convention differs slightly from the previous maps.

The strongest concentration of steep slopes in the San Jose quadrangle occurs in the Diablo Range highlands—Mt. Day and Black Mountain, northeast of the city of San Jose. Another is found on the west side of the Santa Clara Valley, in the Loma Prieta area of the Santa Cruz Mountains. Equally steep slopes occur at much lower elevations, however, such as in the area between Wilcox Ridge and Red Hill, on the eastern slopes of the Diablo Range.

Slope Angle—monochrome (map 11) The same data plotted in color on map 10 are mapped here in continuous tones (0-255), from deep black (zero slope) to bright white (maximum slope). This map reveals two important features not evident in the color plot, bimodality of slope in the San Jose quadrangle and artifacts in the source DEM. The image has very high contrast. Blacks and whites—not gray tones—dominate the map, emphasizing the strong dichotomy between erosional (steep) and depositional (gentle) topography that is characteristic of this young and tectonically active area. The contrast also is evident in the slope histogram (fig. 6), which shows strong modes at one and 13 degrees.

Map 11 also reveals two of the three data-related artifacts that mar this otherwise accurate new DEM (for details see Acevedo, 1991). Both problems reflect incorrect elevations that were incorporated into the DEM during its creation; none of these has been removed from the data set or from the maps shown here. That these maps are as good as they are reveals the overall high signal-to-noise ratio of the new 1:100,000 DEM despite its local shortcomings.

The dark horizontal line passing through the center of the map is a band of unduly similar elevations, and thus low slopes, three to six pixels wide. It reflects the overlapping of similar areas during a suboptimal merging of adjoining panels when the DEM was assembled from constituent subquadrangles. The defect is difficult to repair; at best the erroneous elevations could be only partly restored by modeling the area from adjacent data. The problem could be avoided altogether by processing the entire 1;100,000 quadrangle as one data set.

Star-burst 45-degree light-on-dark patterns appear in low-relief topography, for example, in terrain adjoining interstate route 5 and on the eastern edge of the Santa Cruz Mountains (map 1). These patterns are linear arrays of elevations that are raised slightly but abruptly above the surrounding terrain. The problem stems from deficiencies in the computer software by which digitized hypsography (contours) is converted to a DEM grid. These patterns are more serious than the

subquadrangle-splicing errors and even harder to remove. Currently the worst of them have been edited out of the DEMs manually by NMD personnel, but map 11 shows that many remain. The only effective solution is a more sophisticated gridding algorithm than currently used in DEM production by the USGS (Acevedo, 1991). A third problem of data quality is discussed below, under shaded relief.

Slope Aspect (map 12) Aspect (or azimuth), the compass direction faced by a sloping segment of the ground surface, is the first horizontal derivative of elevation (Evans, 1972). It is useful in studying such determinants of microclimate as exposure of topography to the Sun. Slope-aspect portrays topography more realistically than slope angle (maps 10 and 11) but not as well as shaded-relief (maps 13 and 14). Here, aspect is plotted in 255 continuous tones clockwise from 0 degrees (deep black: due North) to 359 degrees (bright white, nearly due North). As in the case of the elevation-relief ratio (map 9), however, slope aspect loses its meaning in large areas of low-relief, low-sloping topography. This problem can invalidate much of an aspect map; areas in the San Jose quadrangle with less than about 50 m of relief have been masked out (compare map 9).

The mode of presentation adopted for map 12 is rudimentary. First, any circular distribution of the black-to-white tone progression is in part counter-intuitive, particularly near due North. Ideally, light tones should face a simulated Sun placed above the western or northwestern horizon (compare the shaded-relief images, below). Second, slope aspect is more usefully displayed in discrete azimuth-coded color segments (for example, Moellering and Kimerling, 1990). In unpublished experiments, we have found that as few as eight 45-degree segments are effective in mapping slope azimuth from a DEM; in turn, clusters of similarly oriented pixels then delimit terrain facets, sub-basin-sized unit-cells that are suitable for the geomorphic study of erosional topography.

Shaded Relief (maps 13 and 14) A complex derivative of elevation, relief shading equates values of slope angle and aspect, plus the locations of an observer and a simulated Sun, with 255 shades of gray in a computer graphic that resembles a black-and-white aerial photograph (fig. 7; Yoeli, 1965 and 1967; Batson and others, 1975). Shaded relief has many advantages for visualizing topography. Clouds, vegetation, hydrography, and geometric distortion are absent, and image size is limited only by that of the DEM (Thelin and Pike, 1991). Any simulated Sun angle and azimuth can be used. The 255 gray steps are so small that the visual effect is functionally a continuous-tone image. The equation by which shaded relief is generated, the photometric function, has many variants and refinements (Horn, 1981). Its basic form is

$$\mathbf{I} = k_d \, [L \, cos(i)] + A \qquad (2)$$

where

I = intensity of reflectance,
i = angle between the Sun and the slope normal,
k_d = a coefficient describing reflectance of surface material,
L = a scaling factor for the intensity of illumination, and
A = an additive (ambient) light factor.

Two portraits of the San Jose 1:100,000 sheet in shaded relief are shown here, one (map 13) generated by a simulated Sun above the western horizon, the other (map 14) by a Sun from the East. The Sun elevation is 25 degrees in both cases. Steep slopes are black or white, depending on Sun-facing direction; gentle slopes are shades of gray. All the major topographic features of this complex quadrangle are crisply rendered by relief shading. Specific features alluded to above in this report are more clearly depicted here than on the original 1:100,000 hypsography (map 3). Comparison of maps 13 and 14 reveals some remarkable differences in the appearance of the same topography under contrasting illumination. Photointerpretation of the area from shaded-relief images would be best carried out by a set of eight such pictures, one for each direction at 45-degree intervals (for example, Simpson and Anders, 1992). Stereo pairs of shaded-relief images of the quadrangle can be produced digitally in the computer (Batson and others, 1975).

Maps 13 and 14 clearly reveal two of the three problems that we have discovered in this new 1:100,000 DEM. One, the 45-degree star-burst pattern, is the same as observed on the monochrome slope image (map 11). The second, not well seen on other maps in this set, is yet another effect of the contour-to-grid software currently used to compute DEMs—the algorithm tends to interpolate elevations unduly close to digitized contours. The result is a parallel pseudo-contour pattern that appears in shaded-relief images most clearly on long, gentle slopes. The effect is especially well developed here on the west-facing foothills of the Diablo Range just east of the city of San Jose. These incorrect elevations also are clearly evident in histograms of the source DEM as frequency peaks coincident and near-coincident with the contour interval, here 50 m (fig. 4; also Acevedo, 1991). Unpublished work not described here has shown further that the problem is significantly more severe in gentle terrain (slope less than about six degrees), where contours are widely spaced.

Slope Reversals—unfiltered (map 15) Most of the measures mapped by digital techniques in this report describe topography of the San Jose quadrangle in the Z, or vertical domain, rather than the X,Y or horizontal domain. This deficiency reflects a historical trend—evident from the earliest work in morphometry (for summaries, see Neuenschwander, 1944; Carr and Van Lopik, 1962)—to measure the easier (relief) rather than the more challenging (spatial) derivatives of height above sea level. The advent of automated cartography has yet to materially alter this imbalance (Tobler, 1969; Evans, 1972; Pike and others, 1987). The various X,Y attributes of topography, particularly as used to describe ridge and stream segments, are referred to collectively as pattern or texture. These properties include spacing, azimuth direction and strength (that is, its frequency or persistence in the terrain), angularity, parallelism, and contiguity (Nystuen, 1966). We have computed only the most straightforward of these, spacing (or rather its inverse, frequency of slope reversal), for this report.

Slope reversal, or slope-direction change, is defined as a change in ground inclination from uphill to downhill, or vice-versa, along a topographic profile (for example Wood and Snell, 1960) or any rank, file, and/or diagonal of a DEM (fig. 3; Pike, 1988a). By convention the uphill-to-downhill changes, or convexities, are designated positive and the downhill-to-uphill changes, or concavities, are

designated negative. Our computer algorithm records every such change in a DEM in the X and Y directions but not along the diagonals.

Plotting all convexities in erosional topography, such as the upland terrain in most of the San Jose quadrangle, generally results in a web of ridges (shown in red in map 15), whereas plotting the concavities yields a network of drainageways (blue in map 15). Neither of these patterns is an integrated hydrologic or topologic net (although such a net can be derived from a DEM by modeling downhill flow, pixel-by-pixel; for example, Jenson and Domingue, 1988). The lines in map 15 simply convey an overall picture of the drainage pattern and the degree of dissection in the San Jose quadrangle. The natural patterns in low-relief areas, however, are contaminated by the false 45-degree star-burst artifacts encountered in other images, above.

Slope Reversals—filtered (map 16) Most of the spurious star-burst artifacts observed in map 15 have been removed from map 16 (similarly coded in red and blue). We accomplished this by excluding from the recorded concavities and convexities (fig. 3) all slope reversals subtending an angle of less than an arbitrarily chosen (through trial and error) threshold value of three degrees. The excluded changes in terrain slope, most of which reflect local inaccuracies or statistical noise in the DEM rather than real topographic information, are so minor that their removal does not materially change the overall pattern. Where DEMs contain substantial errors, thresholds other than three degrees need to be tested to find the best balance between exclusion of spurious data and real information. However, because filtering removes real data on X,Y attributes, the only information that can be satisfactorily measured from DEMs in very gentle topography, this procedure is just a temporary expedient until better gridding methods are adopted for DEM production.

Thus filtered, the slope-reversal changes remaining in map 16 furnish an improved estimate of ridge and valley spacing created by the San Jose drainage net and its interfluves (albeit incomplete in areas of low relief). Removal of statistical noise by the filtering process also clearly reveals the horizontal edge-matching flaw in the DEM—evident as a band of sparse observations across the middle of the quadrangle, as described earlier for the monochrome slope map (map 11). (The flaw is detectable, but with difficulty, in the unfiltered map 15.)

Frequency of Slope Reversal (map 17) Defined as the inverse of ridge-to-valley spacing, slope-reversal frequency is a function of drainage density—the conventional measure of dissection. Although map 16 provides an intriguing picture of ridge and valley pattern in the San Jose quadrangle, the filtered pattern of slope reversals is only a qualitative assessment of topographic spacing. Map 17, however, provides a quantitative approximation of drainage density. Using the filtered results from map 16, the frequency of occurrence of slope reversal per unit area (one km^2) was computed and mapped in ten intervals. (Map 17 has the same colors as the elevation maps, but the intervals increase in increments of 48 reversals per km^2.) The horizontal DEM-based flaw detected in map 15 also is visible in this map.

The number of slope reversals varies from zero to about 480 per km^2 across the San Jose quadrangle (fig. 8). The frequency distribution is dichotomous, with modes at zero (gray on map 17) and at 240 reversals/km^2 (green and yellow).

Unlike most of the images in this report, map 17 does not visually correlate with elevation—aside from the obvious contrast between erosional (high frequency) and depositional (low frequency) topography.

The fluvial dissection indicated by this measure is particularly strong in such locales as Bollinger and Castle ridges—south of Mt. Hamilton (see map 1), the area south of Pine Springs Hill—northwest of San Luis Reservoir, Garzas Creek—west of Gustine, and Uvas Creek in the Santa Cruz Mountains. Areas of low dissection include Coe State Park and the Coyote Creek drainage, Eylar Mountain—on the northern margin of the map, Poverty Ridge—northeast of San Jose, and terrain just north of Loma Prieta.

Slope Curvature (map 18) Terrain curvature not only indicates the degree of local concavity or convexity in topography, but also is an important measure of surface roughness. Curvature is the second derivative of elevation (Tobler, 1969) and the first derivative of both slope angle (the Z domain) and slope aspect (the X,Y domain). Planimetric (X,Y) curvature is not addressed in this report (see Evans, 1980). In the vertical (Z) domain, an angle of curvature may be measured two ways: first, continuously, pixel-by-pixel and over short distances, at all possible locations along a sampling traverse (*base-length* curvature; fig. 3); second, at wider-spaced locations that separate neighboring terrain facets—that is, hilltops, valley bottoms, and other points of topographic inflection (fig. 3). We have chosen the latter approach, and use *slope reversals* (from map 16) as the specific break-points where curvature is measured.

This method employs an operational expedient that simplifies calculations for DEMs. Our sample design is the so-called rook's case—traverses along which curvatures are computed are the ranks and files (but not diagonals) of a DEM (Pike, 1988a). The resulting values are thus *components* of curvature rather than true values measured in the direction of steepest slope or normal to it. Component values always slightly underestimate the true value, which nonetheless can be estimated statistically (Pike, 1978).

We measured slope curvature at each pixel mapped as a ridge or channel on the filtered image of slope reversals (map 16). As calculated by our algorithm, curvature is the complement of the angle subtended by the pixel containing the reversal and the two pixels containing the nearest reversal on both sides, upslope or downslope, *along the traverse* (fig. 3). The resulting angle is that between opposite-facing slope facets rather than the actual curvature of the slope reversal itself. It is accordingly a simplified measure and is not curvature *strictu sensu*, which would be the radius of a circle or ellipse or curved surface fitted to several elevations straddling each slope reversal (for example, Papo and Gelbman, 1984; Ellen and Mark, 1988).

Values of simple angle of curvature in the San Jose quadrangle range from zero to 105 degrees. Map 18, which divides this spectrum into nine 10-degree or 20-degree bins coded by color, shows all observations of both ridgetop and valley bottom curvature (the two are not separated here) plotted as individual pixels. The resulting colored lines in map 18 enable the more rugged ridges and drainageways to be quickly recognized and quantitatively distinguished from their less rugged counterparts. The horizontal flaw in the DEM, again evident as an area of sparse observations, appears in the curvature map (hard to see in map 18).

Curvature was not quantitatively compared with other measures for this report, but some conclusions may be drawn from inspection. Ridges and valleys that are sharp-crested and steep-walled (curvature values about 60-105 degrees) are common in the San Jose quadrangle, but are less prevalent than rounded ridges and open valleys. The maps indicate that curvature seems to increase markedly with slope angle (maps 10 and 11) and relative relief (map 8), but less so with altitude (maps 4, 5). Some sharp-crested ridges and steep valley bottoms are found in most topographic settings throughout the uplands. Open drainageways and gentle ridgetops (curvature values under 60 degrees), however, clearly are more common at the lower elevations.

Mean Curvature (map 19) Pixel-by-pixel values of slope curvature for individual ridges and valleys in map 18 can be aggregated by larger unit cells for ease of comparison with other generalized maps (for example mean elevation, map 5). We computed average curvature on a 2X2-km window for the San Jose quadrangle, and mapped the result in six ten-degree-intervals (map 19). Averaging appears to have removed the horizontal-band DEM flaw so evident in the more detailed maps, but we caution that any erroneous values in those data also have been incorporated into this map, however generalized. Map 19 describes terrain roughness; in general its pattern resembles those of slope (map 10) and relative relief (map 8).

Map 19 shows that mean angle of curvature for much of the eroding upland in the San Jose quadrangle is about 20 to 30 degrees (orange pattern), and in rare instances over 50 degrees, but less than ten degrees for the alluvial flats (green pattern). This dichotomy is evident in the histogram (fig. 9), which shows curvature modes at about two degrees and 27 degrees. The largest areas of rough topography east of the Santa Clara Valley are found on Mt. Hamilton, on Poverty Ridge to the north of it, and on Wilcox Ridge west of Gustine. Valleys that drain Loma Prieta Ridge in the Santa Cruz Mountains are comparably rough on the western side of the Santa Clara Valley. The Isabel and San Antonio valleys are conspicuously smooth.

TOPOGRAPHIC TYPES, A MULTI-FACTOR MAP (map 20)

Five topographic types in the San Jose quadrangle (fig. 10, map 20) were synthesized from six single-factor maps by the method of numerical taxonomy (Pike, 1972; Pike and Acevedo, 1988; Reichenbach and others, 1992). Our techniques differ from those adapted from Hammond (1964) by Dikau and others (1991) to parse the state of New Mexico. The constituent maps are of elevation (the DEM), relief, slope, the elevation/relief ratio, mean curvature, and slope-reversal frequency. A computerized procedure, cluster analysis (in this case adapted from remote-sensing classification of multispectral images), grouped or separated more than 250,000 samples (every tenth pixel) according to their similarities and differences at the same locations on all six maps. Provisionally, the resulting topographic types are termed high roughland, upper roughland, low roughland, the plains/roughland transition, and lowland plains.

Method The five types were computed from the six maps by an *unsupervised* technique of clustering and classification. That is, the output

image (map 20) was not prefigured by training samples—map locations (pixels) having the characteristics of terrain categories determined beforehand (which is *supervised* clustering; Jensen, 1986). Unsupervised classification, which requires only that the *number* of desired classes (here, five) be specified, is not as Procrustean as the supervised mode, but it is somewhat less objective than the computerized procedure we have used elsewhere to partition smaller data sets (Pike, 1972, 1974; 1988b). the San Jose DEM is so large, however, that only image-processing techniques are efficient enough to rapidly classify the entire quadrangle. We chose five output categories as the most that were likely to represent real differences in San Jose topography.

The six input maps were selected to represent the greatest diversity of topographic characteristics computed by our current programs (Table 1; Pike, 1988a). The results (map 20, figure 10) should be interpreted with limitations of this software in mind. Our measures are the same by which Pike and Acevedo (1988) parsed southern New England and Reichenbach and others (1992) partitioned Italy. They include four of the six criteria used by Wood and Snell (1960) in their study of Central Europe—slope, (maps 10 and 11) relief (map 8), elevation (4), and elevation skewness (map 9), but substitute curvature (map 19) for grain and slope-reversal frequency (map 17) for slope-reversal magnitude. All three of Hammond's (1964) criteria are included here: slope, relief, and profile type (essentially map 9, elevation/relief ratio). These six maps account for three of the five basic attributes emphasized by Evans, (1972, 1980)—elevation, slope, and profile curvature. Our TAP software (Table 1) does not yet include plan (X,Y) curvature and strength of slope aspect.

The clustering and classification algorithms were taken from the EDITOR software package, which was first written by others in the 1970s to generate periodic estimates of agricultural crop acreage from analyses of satellite (Landsat) images. It has evolved into a large general-purpose image-processing system (PEDITOR) with over 100 program modules. This highly portable package is described in a recent land-use application (Hlavka and Sheffner, 1988).

The unsupervised clustering in PEDITOR is a two-step procedure (Swain and Davis, 1978, p. 177-185) that treats each map location, or pixel, as one taxonomic unit. First, a degree of similarity, or taxonomic distance, between each location and every other location—with respect to values for that pixel on all six input maps—is computed statistically in n-dimensional space, where n is the number of input maps. The pixels are then sorted into unique categories (for that n-fold data set and for the number m of output groups specified) according to values of a coefficient of similarity. PEDITOR uses the Euclidean distance function as the grouping criterion (see also, Pike, 1972, 1974). X,Y location does not constrain the grouping. From the descriptive statistics computed for each of m categories by a maximum-likelihood algorithm, the classification procedure in PEDITOR creates a single output image (here, of topographic types, map 20) and summary statistics for the output groups (fig. 10) from the six input maps. We did not test the resulting groups for statistical stability (for an example, see Pike, 1974) other than by studying output images for different numbers of groups (not shown).

The Five Types The characteristics of each topographic type, plotted pixel-by-pixel in map 20, are given in figure 10. These provisional *geometric signatures*

for landform types in the San Jose 1:100,000 quadrangle are simply averaged values of the six measures from which they were derived (Pike, 1988a,b). No error bounds were computed. Figure 10 shows that the dominant contrast among the five types is less one of altitude than roughness—here expressed by the closely covarying measures relief, slope, and curvature. Thus we have not followed the highland-upland-lowland distinction (Wood and Snell, 1960; Hammond, 1964) that is conventional in devising a taxonomy for larger areas such as southern New England (Pike, 1972; Pike and Acevedo, 1988) and Italy (Reichenbach and others, 1992). On the basis of figure 10, we have recognized three first-order types: roughland (yellow, red, and purple on map 20), lowland plains (light blue), and a type intermediate between the two (green).

Roughlands occupy most of the San Jose 1:100,000-scale quadrangle and coincide with the Santa Cruz Mountains and the Diablo Range. They occur at almost all elevations, and we have tentatively recognized three second-order types—high, upper, and low—on the basis of the contrasts in average elevation shown in figure 10. Distinctions among the three subtypes are minor, and are not visually conspicuous in either the physiography (maps 13 and 14) or in the hypsography (map 3). Some contrast between high roughland and the other two roughland types can be detected in the four plots of elevation (maps 4-7), but none is evident in slope angle or other measures. Only maximum elevation (map 6) suggests some distinction between low and upper roughland.

The modest topographic contrasts in the roughlands are more evident analytically than visually. For example, the signatures diagram (fig. 10) shows that mean local relief is highest in the high roughland (750 m), but that intricacy of dissection—slope-reversal frequency (225/km^2)—is not (at 300/km^2, terrain features are more closely spaced in upper roughland). Otherwise, high roughland closely resembles upper roughland—in slope, curvature, and elevation/relief (fig. 10). Upper and low roughland are identical in relief, and the two are similar in slope and curvature; other differences between these two types mimic those of relief in figure 10. Topographic contrasts within the roughlands may be too small to reflect distinctions in geologic interpretation (all three types are subject to intense erosion), pending assurance that a statistically stable classification of topography has been achieved—perhaps through further experimentation with refined techniques of cluster analysis.

The geometric signature of lowland plains, the next most prevalent first-order type, contrasts dramatically with that of the roughlands. Values of all five descriptive properties in figure 10 (elevation/relief, map 9, is indeterminate) are uniformly low—local relief (map 8) rarely exceeds 25 m or slope angle (map 10) 5 degrees. Maximum elevation (map 6) is almost always less than 100 m. Our measures are not sufficiently sensitive to detect whatever subtle topographic differences may exist between the Santa Clara and San Joaquin valleys. Maps 13 and 14 show the lowland plains to be bland and virtually featureless save where they approach the transition to roughland. The plains topographic type hosts rapid sedimentation in both major valleys.

The plains-roughland transition, the least common of the three main types in the San Jose quadrangle, is characterized by intermediate to low values of all measures. Comparison of map 20 with constituent maps reveals that elevation maxima of roughly 130-260 meters (map 6), mean curvatures of 10-20 degrees (map 19) and a slope-reversal frequency of about 100-250 are conspicuously

prevalent in this type. The low elevation/relief mean of 0.27, which is to be expected for borderland topography separating contrasting topography, is so much less than values for the other four types that it is virtually diagnostic. The low to moderate values of all five other descriptors of this topographic type (fig. 10) are consistent with its geographically intermediate location between roughlands and plains and a mixed-process geomorphic regime where erosion, although perhaps the dominant process, is far less vigorous than in the roughlands.

Spatial Units Individual pixels classified statistically into one of five types in the San Jose 1:100,000 quadrangle (fig. 10) also cluster spatially (map 20). This areal coherence is remarkable in the absence of any conversion of the original measures into principal components—a transformation that simplifies input data by collapsing them into orthogonal (uncorrelated) synthetic variables—thereby removing undue weighting of the classification procedure by highly related measures (Pike, 1972, 1988a, b). Additional digital images computed for this area by the same technique (not shown), the results of specifying three and four topographic types for the clustering, also resemble map 20—particularly in the clear-cut separation of alluvial from erosional topography and in one case the presence of a transitional belt between them. Despite this suggestion of statistical stability, our attempt to delimit spatial units remains preliminary and exploratory.

The spatial clustering suggests that at least some of the five types of topography could reflect such areally restricted contrasts in geologic processes and events that physiographic units might be delimited from them. To address this question we compared topographic types (map 20) with geologic units (both map 2 and Wagner and others, 1991), by overlays, and looked for close correlation of geologic units with the putative topographic subdivisions. The results of this qualitiative comparison, described below for each type, are mixed and in some cases ambiguous. We similarly compared our topographic types with the aeromagnetic map of the San Jose area (not shown) compiled by Abrams (1992), but identified no correlations.

The lowland plains type is the most uniform of the five in its geologic makeup; it corresponds closely to the widespread occurrence of many Quaternary deposits, largely alluvium, in the Santa Clara and San Joaquin Valleys (map 2). Other, usually older, Quaternary units are incorporated into the plains where they border the transition type of topography. If any of the five types warrants designation as a physiographic unit, or perhaps two units representing the two valleys, it is this one.

The transition type is more heteogeneous in its geologic composition than the plains. This variety mirrors the physiographic diversity that arises from the presence of both upland and plains terrain within this type; the bordering alluvial fans are perhaps its dominant topographic characteristic (maps 13 and 14). Along the western San Joaquin Valley, the transition type includes Tertiary marine sedimentary rocks—most conspicuously the Tesla Formation (Wagner and others, 1991), plus some Quaternary units and Cretaceous marine rocks at lower elevations. Along the western margin of the Santa Clara Valley, the transition type tends to include Franciscan material, whereas along the eastern margin the type comprises both alluvial and non-alluvial Quaternary deposits and incorporates some Cretaceous and Tertiary-Cretaceous marine rocks and

ultramafics. This topographic type also is found in several upland valleys. Despite the distinctiveness of this type in figure 10, we question that it has enough lithologic uniformity and spatial coherence (map 20) to be useful as a physiographic unit.

The geologic makeup of the roughland type is highly variable, even within each of its three subtypes. Only in the Diablo Range does the high roughland bears any evidence of a systematic terrain-lithology correspondence, where it is conspicuously restricted to the upper elevations of the Franciscan Assemblage with only minor contributions from ultramafics and Tertiary-Cretaceous marine rocks (map 2). At lower elevations, however, the same rocks also host the other two types of roughland. In the Santa Cruz Mountains, the high roughland type is developed on a great variety of Cenozoic marine rocks, plus some Franciscan materials at higher elevations.

The upper and low roughland types, taken separately, are not systematically distributed according to rock type in either the Santa Cruz Mountains or the Diablo Range save for some suggestion that the sandstone, shale and conglomerate facies of the Franciscan Assemblage tends to underlie upper rather than high roughlands (Wagner and others, 1991). Both lower-elevation types host a great variety of rock units. Taken together, with low roughland predominating, these two types do include virtually all of the Upper Cretaceous Berryessa Formation in the area (Wagner and others, 1991), but otherwise do not correlate significantly with geology. Of the five topographic types distinguished in figure 10, upper and low roughland are the least convincing in map 20. We conclude that high roughland is the most distinctive type of topography after the lowland plains, but that a valid physiographic unit probably would comprise more than just this one subtype.

In sum, no more than three of the five topographic types identified in the San Jose 1:100,000 quadrangle by digital techniques (fig. 10) are sufficiently correlated with lithology or selective proximity to faults (map 20) to define physiographic map units in the generally accepted sense. We did not find any systematic relation of topographic types to aeromagnetics. The occurrences of the lowland plains type delimit the most distinctive terrain unit; given the data described here, one or perhaps two non-plains topographic units also appear reasonable. Correspondence of the terrain types with landslide occurrences and habitats, neither of which has been mapped in this area, and other geologic features remains to be evaluated. Nor have we closely compared patterns on our individual thematic maps with the location of specific geologic features. Another approach to evaluating prospective physiographic divisions, which lies beyond the scope of this report, is to use the computer to quantitatively compare digital maps of the geologic units with those of the provisional topographic units and their constituent measures of terrain form.

DISCUSSION AND RECOMMENDATIONS

The work described here is preliminary in several respects. The landform types in map 20 and the various digital maps from which they are derived could be manipulated further in applications that are both geologic (for example, Colleau and Lenôtre, 1991; Simpson and Anders, 1992) and only indirectly geologic. Among the latter are derivation of eco-regions and related spatial classifications

for land-use zoning and policymaking, hazard and risk analysis, benefit-cost modeling, and various environmental needs—both in the San Jose area and elsewhere (Bernknopf and others, 1988; Ellen and Mark, 1988; Wentworth and others, 1991). These applications can be achieved by comparing or combining digital topography with such mapped variables as rock and soil type, hydrology, climate, vegetation, demography, existing land use, and occurrences of specific natural hazards (for example, landslides). In the San Jose quadrangle, only some of this information currently is available in digital map format whereby it can be readily registered with topographic data.

One of the most most pressing problems to be examined in subsequent study is better description, a need currently shared by all DEM-based analyses of topographic form. The input measures available from the current version of our software package (TAP) do not adequately characterize the X,Y dimension: topographic pattern (Table 1; see discussion of map 15). This shortcoming could be remedied by programming into TAP such parameters of terrain texture as topographic grain—a measure of spatial autocorrelation (Wood and Snell, 1960; Pike and others, 1989), the direction and strength of slope azimuth (Evans, 1972; Pike and others, 1987), an estimate of planimetric curvature (Evans, 1972, 1980), and some descriptor of ridge and valley topology (Mark, 1988). Extracting these attributes from DEMs is computationally more demanding than the measures shown in maps 5-19.

A major issue that arises from our work and needs to be addressed in depth is the probable scale-dependence of terrain characteristics and any taxonomy resulting from their manipulation. We think that the distinctiveness of topographic units varies inversely with the extent of the area under study. For example, our provisional topographic types and units in the comparatively small San Jose sheet are not as crisply defined as those derived by the same approach for the much larger areas of central Europe (Wood and Snell, 1960; Pike, 1986), southern New England (Pike, 1972; Pike and Acevedo, 1988), and Italy (Reichenbach and others, 1992). Aside from the obvious and general dichotomy between alluvial lowland and dissected upland, terrain units in the San Jose sheet do not mirror strong contrasts in lithology and structural style. This low correspondence may simply reflect the quadrangle's location within a single physiographic province—which in turn suggests that a spatial classification of terrain may make the most sense in large and diverse regions (Hammond, 1964; Dikau and others, 1991). On the other hand, the criteria that successfully parse a large region may be unsuited for subdividing a smaller one. The latter alternative suggests that topographic measures other than those in maps 4-19 are needed if topographic samples as small as 1:100,000-scale map sheets are to be analyzed in this way.

A more process-oriented approach to the problem of regional topographic analysis by DEM would broaden the geomorphic and tectonic implications of the work described here (for example, Colleau and Lenôtre, 1991; Simpson and Anders, 1992). One way to do this is to transform the continuously distributed elevation data to landform-specific (discrete) spatial units, most probably through a DEM-to-watershed computation (for example, Band, 1986; Jenson and Domingue, 1988). We caution, however, that the success of such network analysis depends upon solutions to the software problems that allow so much error to enter current 1:100,000-scale DEMs.

Another area that remains to be addressed in greater detail is the combination of digital images into a spatial taxonomy of topographic units. This is a complex statistical problem, and the somewhat "black-box" computations of the PEDITOR package used here do not accommodate as much step-by-step monitoring of the process as might be desired. Experience has shown that the best results from automated classification are obtained by observing several guidelines (Pike, 1974; 1988a): (1) choosing input variables that both measure different constituents of topographic form and include as many key attributes of the landscape as possible, (2) using relatively symmetric input distributions (paying particular attention to eliminating outliers)—commonly achieved by transformations of the raw measures, (3) preceding the classification by a principal-components analysis to both simplify the input data through reduction of internal correlation and to rank them in order of importance, (4) carrying out the classification on the resulting components—weighted by their relative importance, and (5) evaluating the classification by studying a linkage diagram (dendrogram) as well as an output image (here, map 20). These steps will not guarantee a robust system of topographic units, but stable results are unlikely without them.

Two important implications of our work that are addressed only incidentally in this report are error-detection and quality control of the elevation data (Acevedo, 1991; Crosley and Boucher, 1991). Although all DEMs generated by the U.S. Geological Survey satisfy conventional map-accuracy standards, those criteria were designed explicitly for contour maps and as currently configured are not effective in removing at least three kinds of error from digital elevation data. Several of our maps reveal such errors in the San Jose 1:100,000 DEM, and the higher the DEM derivative the more sensitive the resulting map is to those errors. Accordingly, we recommend that inspection of such digital images as slope, shaded-relief, and slope reversal be introduced as a routine quality-control procedure for checking DEMs during their production and before publication.

CONCLUSIONS

The efficiencies of digital image-processing have enabled us to create thematic maps that variously represent or classify large areas of topography in a remarkably short time. The computer methods applied in this report to a moderate-resolution 2,000,000-pixel DEM yield a variety of image maps and quantitative characterizations of the San Jose area. The fine detail evident in several of these color and monochrome maps can not be attained economically in small-scale graphics made of similarly large areas by pictorial relief, airbrush, plastic raised-relief models, and other nondigital means. The multivariate technique by which terrain types and units are synthesized statistically from several constituent maps carries much potential for rapidly analyzing topography, although it may be better suited to areas larger than the San Jose 1:100,000-scale map sheet. The new maps and the digital data they represent have many practical applications that remain to be explored in depth.

This report has identified several areas of likely advance in the numerical analysis of synoptic topography by the techniques of digital image-processing. These issues apply to both the 1:100,000-scale San Jose quadrangle and elsewhere. The most important problems for future study include conversion of geologic and

other map information to digital format for comparison with topography, improvement in terrain characterization—with special reference to spatial variables, detailed experimentation with discrete-unit sampling, a more transparent approach to the clustering procedure, the numerical evaluation of topographic types and spatial units, a better understanding of the scale-dependence of terrain characteristics, further development of our C-language TAP software, the quantitative (computer) comparison of digital maps of topographic measures, and the urgent need for further reducing error in mass-produced digital elevation models.

ACKNOWLEDGMENT We appreciate suggestions by Carl Wentworth that contributed to this report.

REFERENCES CITED

Abrams, G.A., 1992, Aeromagnetic map of the San Jose area, California: U.S. Geological Survey, Miscellaneous Field Studies, map MF-2191, 1:100,000-scale.

Acevedo, William, 1991, First assessment of U.S. Geological Survey 30-minute DEMs: A great improvement over existing 1-degree data, *in* American Society for Photogrammetry and Remote Sensing—American Congress on Surveying and Mapping annual convention, Baltimore, March 25-29, 1991, Technical Papers, v. 2 (Cartography and GIS/LIS), p. 1-12.

Bailey, E.H., ed., 1966, Geology of northern California: San Francisco, California Division of Mines and Geology, Bulletin 190, 508 p.

Batson, R.M., Edwards, Kathleen, and Eliason, E.M., 1975, Computer-generated shaded-relief images: U.S. Geological Survey Journal of Research, v. 3, no. 4, p. 401-408.

Bernknopf, R.L., Campbell, R.H., Brookshire, D.S., and Shapiro, C.D., 1988, A probabilistic approach to landslide hazard mapping in Cincinnati, Ohio, with applications for economic evaluation: Bulletin of the Association of Engineering Geologists, v. 25, no. 1, p. 39-56.

Brabb, E.E., 1987, Analyzing and portraying geologic and cartographic information for land-use planning, emergency response, and decisionmaking in San Mateo County, California, *in* American Society for Photogrammetry and Remote Sensing—American Congress on Surveying and Mapping, International Conference, Exhibits, and Workshops on Geographic Information Systems, 2nd, GIS '87-San Francisco, October 26-30, 1987, Proceedings, v. 1, p. 362-374.

Burrough, P.A., 1986, Principles of geographical information systems for land resources assessment: Oxford, Clarendon Press, 193 p.

Carr, D.D., and Van Lopik, J.R., 1962, Terrain Quantification Phase I, Surface Geometry Measurements: Dallas, Texas Instruments Co., for U.S. Air Force Cambridge Research Laboratories, Report No. 63-208 (Contract No. AF 19(628)-481 Project No. 7628 Task No. 762805), 85 p. plus appendices (including 348-entry annotated bibliography).

Colleau, A., and Lenôtre, N., 1991, A new digital method for analysis of neotectonics applied to the Bonnevaux-Chambaran area, France: Tectonophysics, v. 194, no. 3, p. 295-305.

Crosley, K.R. (with Don Boucher), 1991, Quality control of data through scientific visualization: Scientific Computing and Automation, v. 7, no. 11, p. 45-48.

Dangermond, Jack, 1986, The software toolbox approach to meeting the users' needs for GIS analysis, *in* American Society for Photogrammetry and Remote Sensing, Geographic Information Systems Workshop, Atlanta, Georgia, April 1-4, 1986, Proceedings, p. 66-75.

Dikau, Richard, Brabb, E.E., and Mark, R.K., 1991, Landform classification of New Mexico by computer: U.S. Geological Survey Open-file Report 91-634, 15 p.

Drummond, R.H., and Dennis, H.W., 1968, Qualifying relief terms: The Professional Geographer, v. 20, no. 5, p. 326-332.

Ellen, S.D., and Mark, R.K., 1988, Automated modeling of debris-flow hazard using digital elevation models (abs.): Eos, Transactions of the American Geophysical Union, v. 69, no. 16, p. 347.

Evans, I.S., 1972, General geomorphometry, derivatives of altitude and descriptive statistics, *in* Chorley, R.J., ed., Spatial Analysis in Geomorphology: New York, Harper and Row, p. 17-90.

_____1980, An integrated system of terrain analysis and slope mapping: Zeitschrift für Geomorphologie, Supplementband 36, p. 274-295.

Fitzgibbon, T.T., Wentworth, C.M., and Showalter, P.K., 1991, Digital compilation of geologic maps and data bases using ALACARTE-ARC/INFO (abs.): Geological Society of America, 1991 Abstracts with Programs, v. 23, no. 2, p. 25.

Hammond, E.N., 1964, Analysis of properties in land form geography: an application to broad-scale land form mapping: Annals of the Association of American Geographers, v. 54, no. 1, p. 11-19 and map at 1:5,000,000.

Hlavka, C.A., and Sheffner, E.J., 1988, The California Cooperative Remote Sensing Project: Final Report, Moffett Field, California, Ames Research Center, NASA Technical Memorandum TM-100073, 98 p.

Horn, B.K.P., 1981, Hill shading and the reflectance map: Proceedings of the Institute of Electrical and Electronic Engineers, v. 69 , no. 1, p. 14-47.

Jensen, J.R., 1986, Introductory digital image processing—a remote-sensing perspective: Englewood Cliffs, N.J., Prentice-Hall, 379 p.

Jenson, S.K., and Domingue, J.O., 1988, Extracting topographic structure from digital elevation data for geographic information system analysis: Photogrammetric Engineering and Remote Sensing, v. 54, no. 11, p. 1593-1600.

Kennie, T.J.M., and McLaren, R.A., 1988, Modelling for digital terrain and landscape visualization: Photogrammetric Record, v. 12, no. 72, p. 711- 745.

Mark, D.M., 1978, Concepts of "data structure" for digital terrain models: Digital Terrain Models (DTM) Symposium, May 9-11, 1978, St. Louis, Missouri, American Society of Photogrammetry, Proceedings, p. 24-31.

_____1988, Network models in geomorphology, *in* Anderson, M.G., ed., Modelling Geomorphological Systems, New York, John Wiley and Sons, p. 73-97.

Mark, R.K., and Aitken, D.S., 1990, Shaded-relief topographic map of San Mateo County, California: U.S. Geological Survey Miscellaneous Investigations Map I-1257-K, scale 1:62,500.

Mays, R.R., 1966, Production of numerical maps, *in* Conference—Numerical Topographic Data and Other New Map Products, Fort Belvoir, Va., May 3-5, 1966, Proceedings: Washington, D.C., Department of the Army, Office of the Chief of Engineers, p. 38K-41K.

Moellering, Harold, and Kimerling, A.J., 1990, A new digital slope-aspect display process: Cartography and Geographic Information Systems, v. 17, no. 2, p. 151-159.

Neuenschwander, Gustav, 1944, Morphometrische Begriffe, Eine kritische Übersicht auf Grund der Literatur (in German): Universität Zürich, Inaugural-Dissertation, 135 p.

Nystuen, J.D., 1963, Identification of some fundamental spatial concepts: Papers of the Michigan Academy of Science, Arts, and Letters, v. 48, p. 373-384. [reprinted *in* Berry, B.J.L., and Marble, D.F., eds., 1968, Spatial Analysis, A Reader in Statistical Geography: Englewood Cliffs, N.J., Prentice-Hall, p. 35-41.]

Pannekoek, A.J., 1967, Generalized contour maps, summit level maps, and streamline surface maps as geomorphological tools: Zeitschrift für Geomorphologie, v. 11, no. ?, p. 169-182.

Peucker, T.K., Fowler, R.J., Little, J.J., and Mark, D.M., 1978, The triangulated irregular network: Proceedings of the Digital Terrain Models (DTM) Symposium, American Society of Photogrammetry, p. 516-540.

Pike, R.J., 1972, Q-mode landform regions of southern New England, *in* Adams, W.P., and Helleiner, F.M., eds., International Geography 1972, Papers Submitted to the 22nd International Geographical Congress, Montreal, Canada, Univ. Toronto Press, p. 365-367.

_____1974, Craters on Earth, Moon, and Mars: multivariate classification and mode of origin: Earth and Planetary Science Letters, v. 22, no. ?, p. 245-255.

_____1988a, The geometric signature: quantifying landslide-terrain types from digital elevation models: Mathematical Geology, v. 20, no. 5, p. 491-511.

_____1988b, Toward geometric signatures for geographic information systems: International Geographic Information Systems Symposium—The Research Agenda, Arlington, Va., November 15-18, 1987, Proceedings: Washington, D.C., NASA, v. III, p. 15-26.

Pike, R.J., and Wilson, S.E., 1971, Elevation-relief ratio, hypsometric integral, and geomorphic area-altitude analysis: Geological Society of America Bulletin, v. 82, no. 4, p. 1079-1084.

Pike, R.J., Thelin, G.P., and Acevedo, William, 1987, A topographic base for GIS from automated TINs and image-processed DEMs, *in* American Society for Photogrammetry and Remote Sensing / American Congress on Surveying and Mapping, International Conference, Exhibits, and Workshops on Geographic Information Systems, 2nd, GIS '87-San Francisco, October 26-30, 1987, Proceedings, v. 1, p. 340-351.

Pike, R.J., and Acevedo, William, 1988, Image-processed maps of southern New England topography (abs.): Geological Society of America Abstracts with Programs, v. 20, no. 1, p. 62.

Pike, R.J., Acevedo, William, and Card, D.H., 1989, Topographic grain automated from digital elevation models, *in* American Society for Photogrammetry and Remote Sensing—American Congress on Surveying and Mapping, Auto-Carto 9 Convention, Baltimore, Md., Proceedings, p. 128-137.

Reichenbach, Paola, Acevedo, William, Mark, R.K., and Pike, R.J., 1992, Landforms of Italy: Consiglio Nazionale delle Ricerche, Instituto di Ricerca per la Protezione Idrogeologica nell'Italia Centrale, Perugia, Italy, *in collaboration with* U.S. Geological Survey, scale 1:1,200,000.

Rogers, T.H., compiler, 1966, San Jose sheet, *in* Jenkins, O.P., ed., Geologic Map of California, 1:250,000.

Simpson, D.W., and Anders, M.H., 1992, Tectonics and topography of the western United States—an application of digital mapping: GSA Today, v. 2, no. 6, p. 117, 118, 120, 121.

Smith, G.-H., 1935, The relative relief of Ohio: The Geographical Review, v. 25, no. 2, p. 272-284.

Stearns, R.G., 1967, Warping of the Western Highland Rim peneplain in Tennessee by ground-water sapping: Geological Society of America Bulletin, v. 78, no. 9, p. 1111-1124.

Strahler, A.N., 1952, Hypsometric (area-altitude) analysis of erosional topography: Bulletin of the Geological Society of America, v. 63, no. 11, p. 1117-1142.

Swain, P.H., and Davis, S.M., eds., 1978, Remote Sensing: The Quantitative Approach: New York, McGraw-Hill International, 396 p.

Thelin, G.P., and Pike, R.J., 1991, Landforms of the conterminous United States—A digital shaded-relief portrayal: U.S. Geological Survey Miscellaneous Investigations Map, I-2206, scale 1:3,500,000.

Tobler, W.R., 1969, An analysis of a digitalized surface, *in* Davis, C.M., A study of the land type: Ann Arbor, University of Michigan Department of Geography, Final Report on Contract No. DA-31-124-ARO-D-456, p. 59-83.

U.S. Geological Survey, 1969, NJ 10-9, San Jose, Western United States 1:250,000-scale series (topographic). [revised version of 1962 map by U.S. Army Topographic Command, Washington, D.C.]

_____1978, San Jose quadrangle, 1:100,000-scale series (topographic).

_____1990, Digital elevation models, data users guide 5 (2nd printing, revised): Reston, Virginia, National Mapping Program, Technical Instructions, 51 p.

Wagner, D.L., Bortugno, E.J., and McJunkins, compilers, 1990, Geologic map of the San Francisco-San Jose quadrangle: California Department of Conservation, Division of Mines and Geology, Regional geologic map series, Map no. 5A (geology), scale 1:250,000.
Wentworth, C.M., and Blake, M.C. Jr., 1991, Preliminary geologic map of the San Jose 1:100,000 quadrangle, California (abs.): Geological Society of America Abstracts with Programs, v. 23, no. 2, p. 108.
Wood, W.F., and Snell, J.B., 1960, A quantitative system for classifying landforms: Natick, Mass., U.S. Army Quartermaster Research and Engineering Center, Technical Report EP-124, 20 p.
Yoeli, Pinhas, 1965, Analytical hill shading (A cartographic experiment): Surveying and Mapping, v. 25, no. 4, p. 573-579.
_____1967, The mechanisation of analytical hill shading: Cartographic Journal, v. 4, no. 2, p. 82-88.

Table 1

Terrain Analysis Package (TAP)*

Programs developed to create and manipulate gridded topographic data sets in the San Jose 1:100,000 sheet (not all functions were used for this report)

Shaded relief
Slope angle
Mean elevation within a moving window
Maximum elevation within a moving window
Minimum elevation within a moving window
Local relief (maximum—minimum elevation)
Hypsometric integral (the elevation/relief ratio)
Slope reversals along DEM ranks and files
Frequency of slope-direction change (SDC), or slope reversal)
Adjust SDC image for slope (filter out low-value changes)
Slope direction change (DEM ranks only)
Slope curvature at slope reversals
Elevation skewness
Azimuth trend and vector magnitude within moving window
Topographic grain
Log elevation
Square root of elevation

*The Terrain Analysis Package is a series of software modules written in the 'C' programming language by William Acevedo in collaboration with R.J. Pike. The TAP software runs under the Unix operating system on Silicon Graphics and Sun workstations. This package is under development (several of the modules are still incomplete) and is not yet ready for distribution.

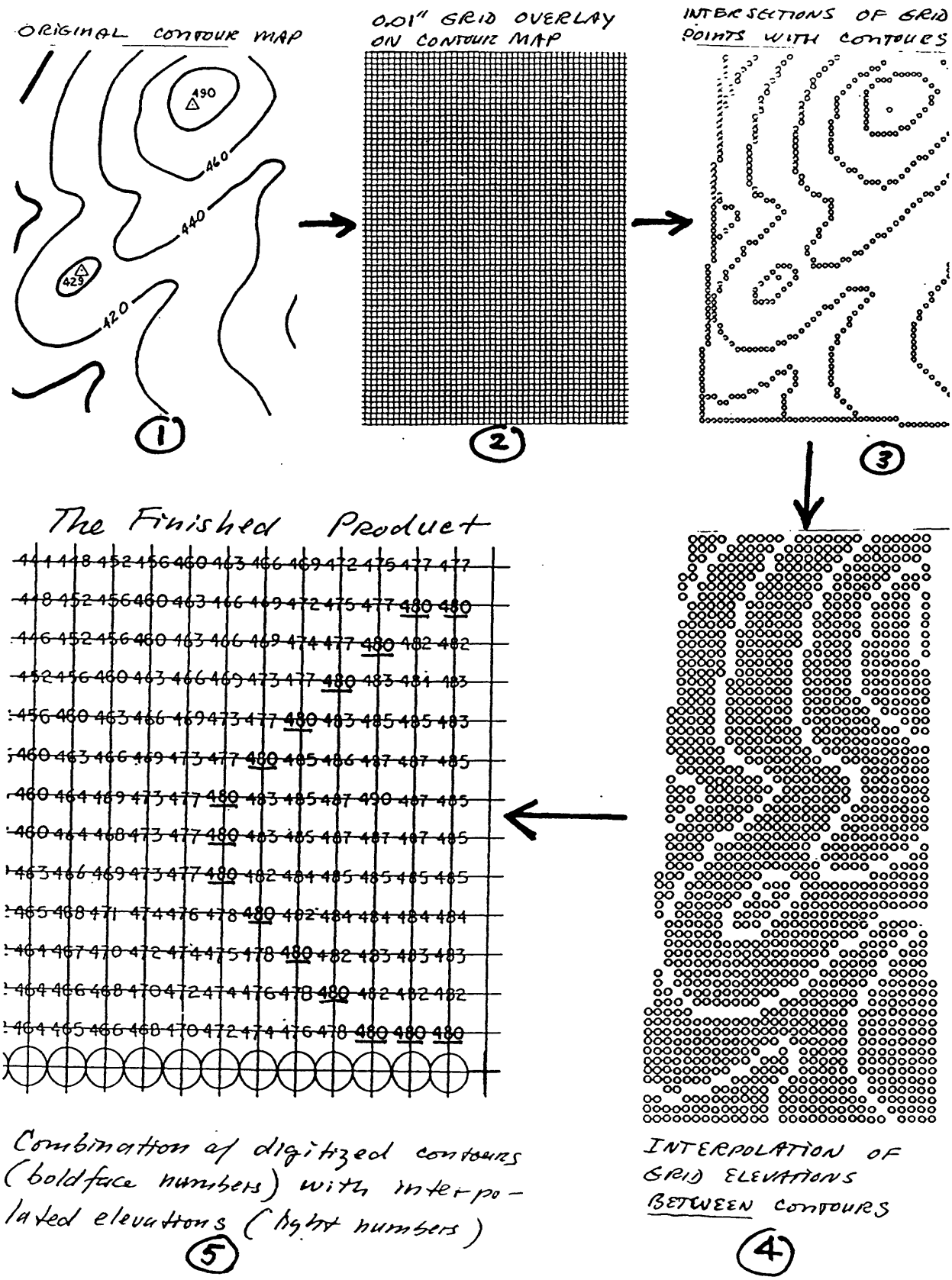

Fig. 1. Principal steps in creating a DEM from a contour map (diagrams show 1:250,000-scale U.S. data; after Mays, 1966). Hypsography of the 1:100,000-scale San Jose quadrangle (map 3) was processed similarly

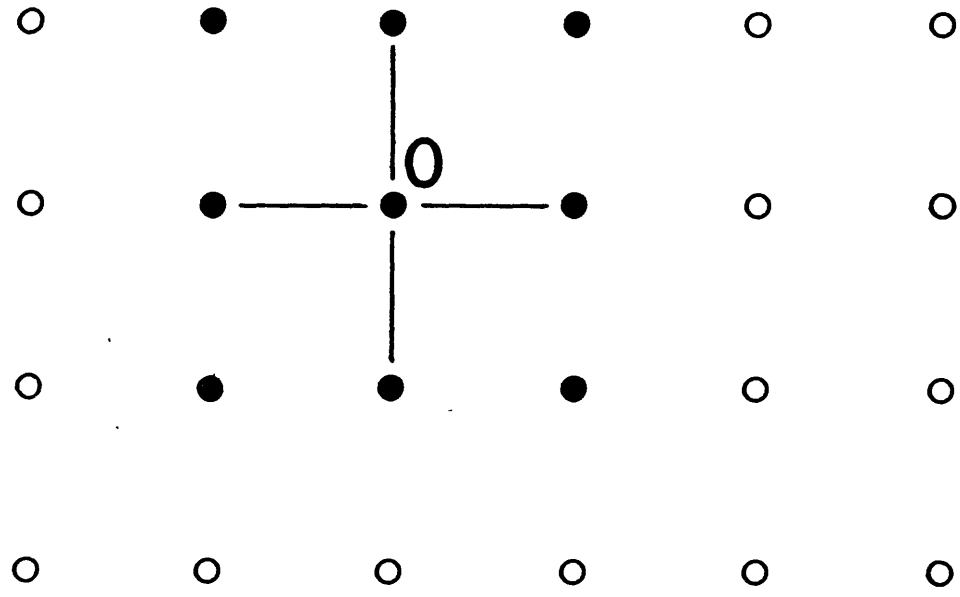

Fig. 2. A 24-point DEM containing a nine-point moving-window sample, or subgrid, used to compute slope angle (maps 10 and 11), slope aspect (map 12), and shaded relief (maps 13 and 14); after Mark and Aitken, 1990; and Thelin and Pike, 1991. Central point, 0, of window is that indicated in figure 7

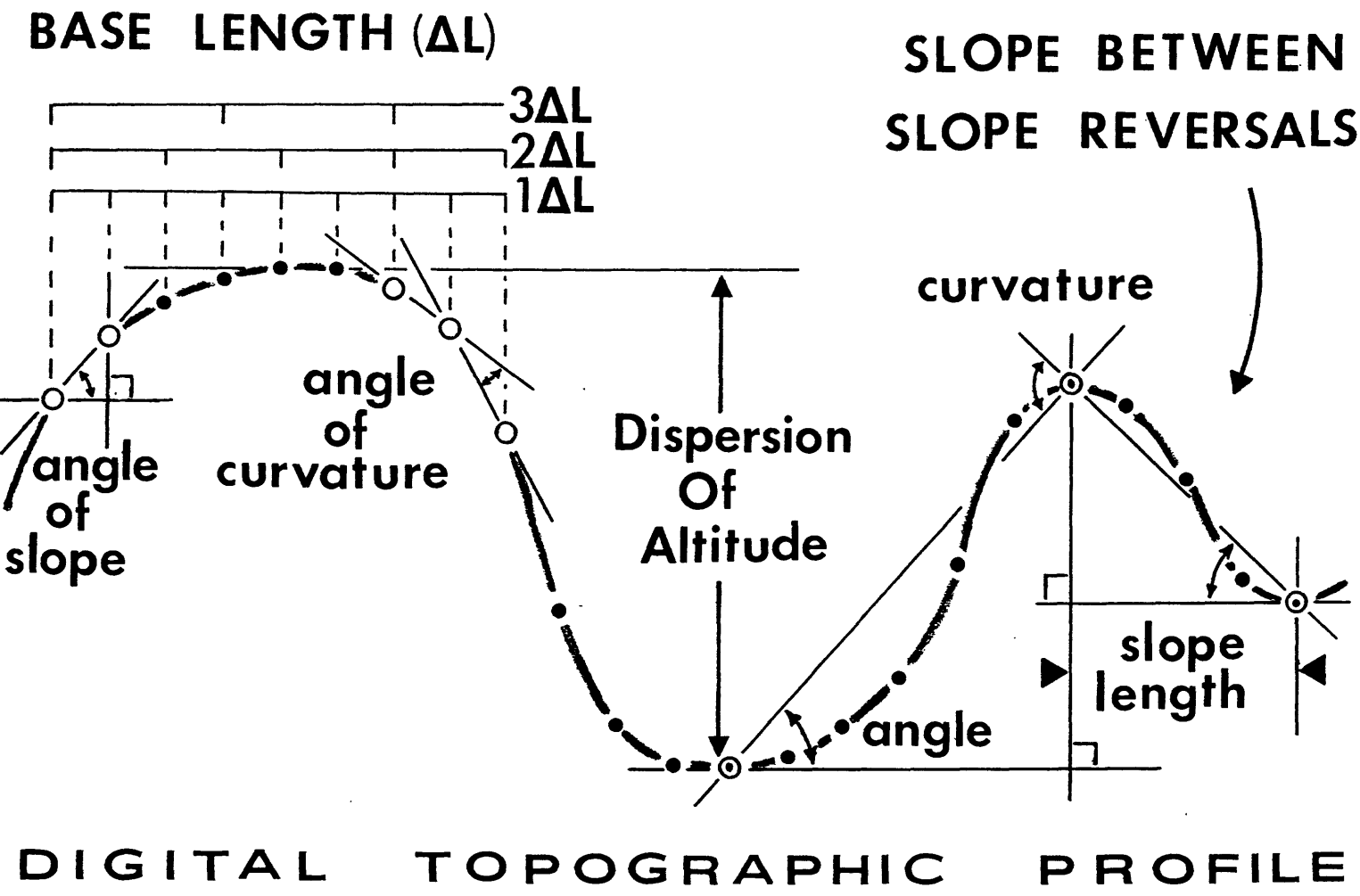

Fig. 3. Examples of topographic measures defined for calculation from DEM ranks, files, and diagonals (after Pike, 1988a, b). Dots and circles are gridded elevations that make up the digital topographic profile; open circles are elevations used to compute measures. Analogous computations for areal (non-profile) samples are more complex (see text for definitions of specific measures used in this report)

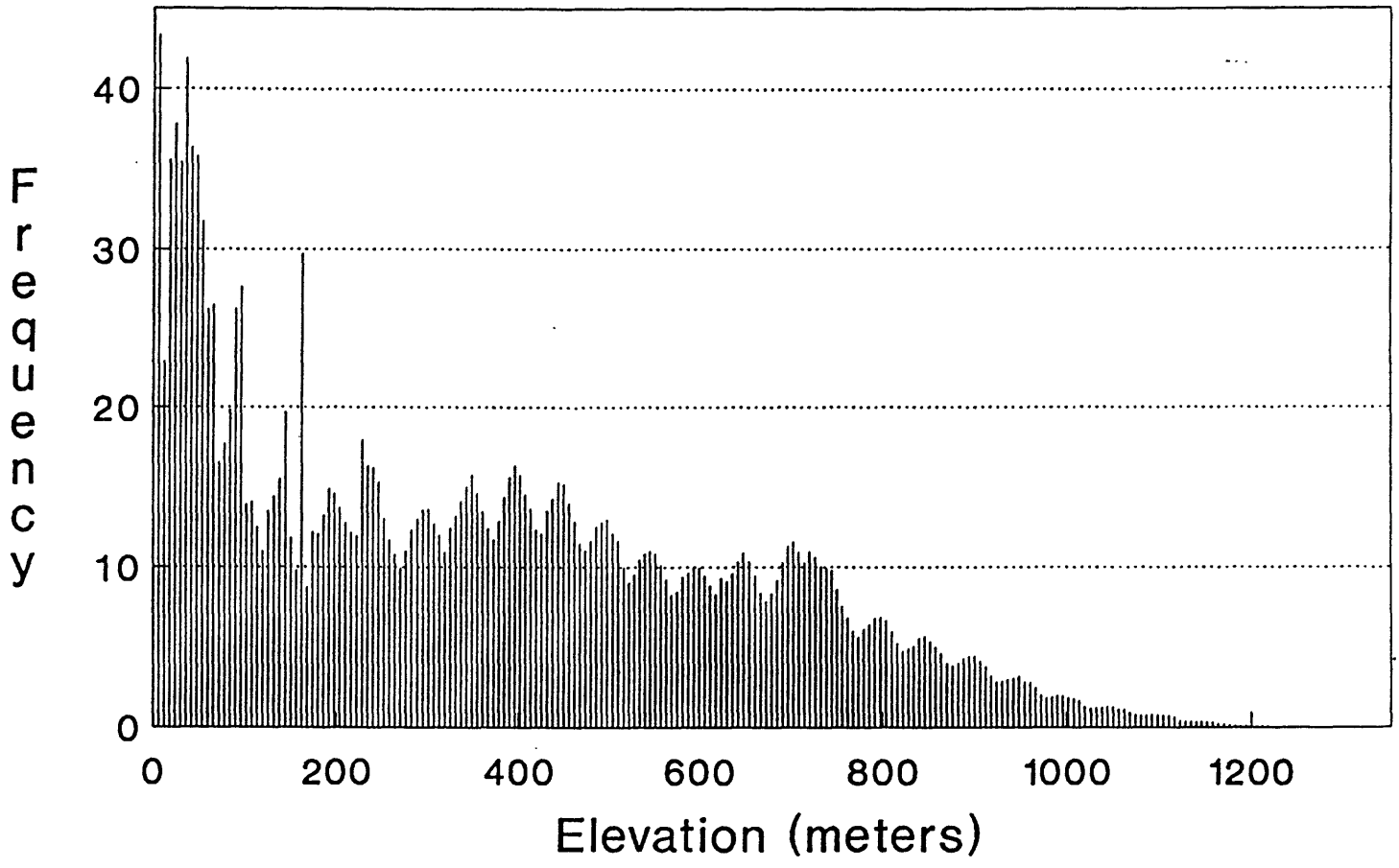

Fig. 4. Histogram of elevation (map 4) for the 1:100,000-scale San Jose DEM (after Acevedo, 1991). Peaks at 50-m intervals are errors, artifacts of DEM derivation from 50-m contour lines, not real terraces in the topography (see discussion in text)

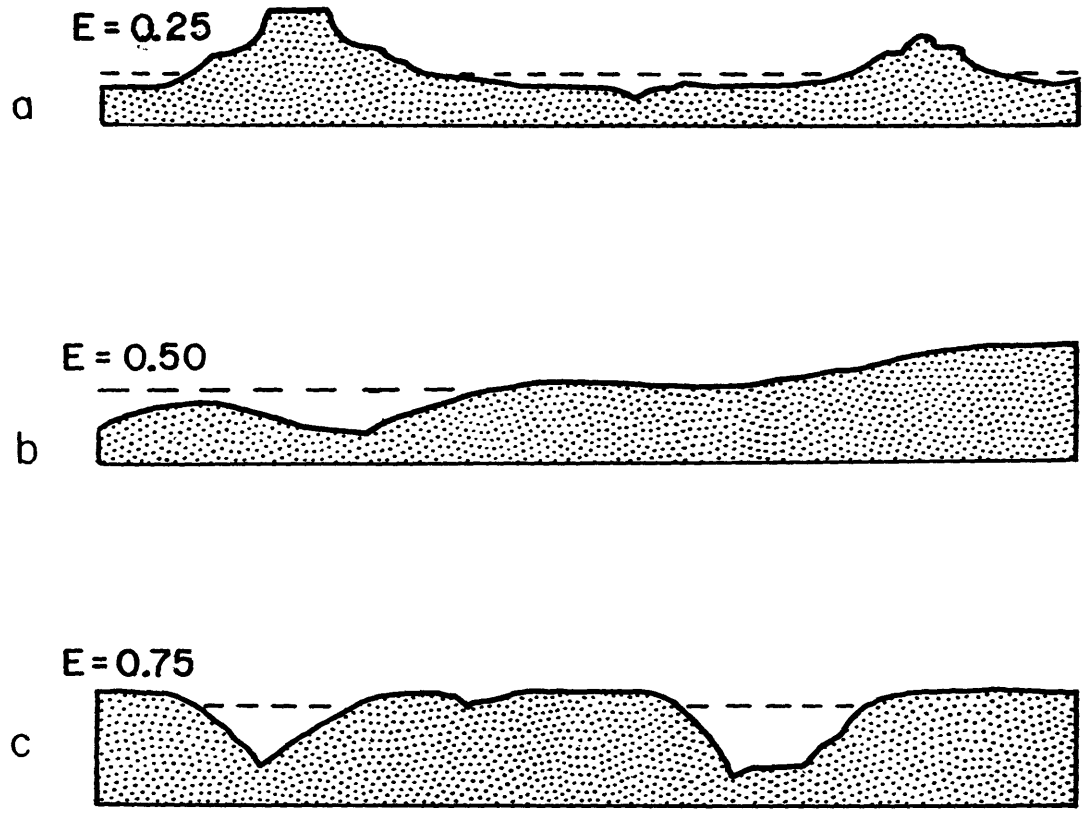

Fig. 5. Relation between skewness of elevation (numbers) and topographic form. Values of the elevation-relief ratio **E** (map 9) computed for three contrasting (fictitious) terrain profiles. Dashed line is mean elevation (see text discussion and equation 1)

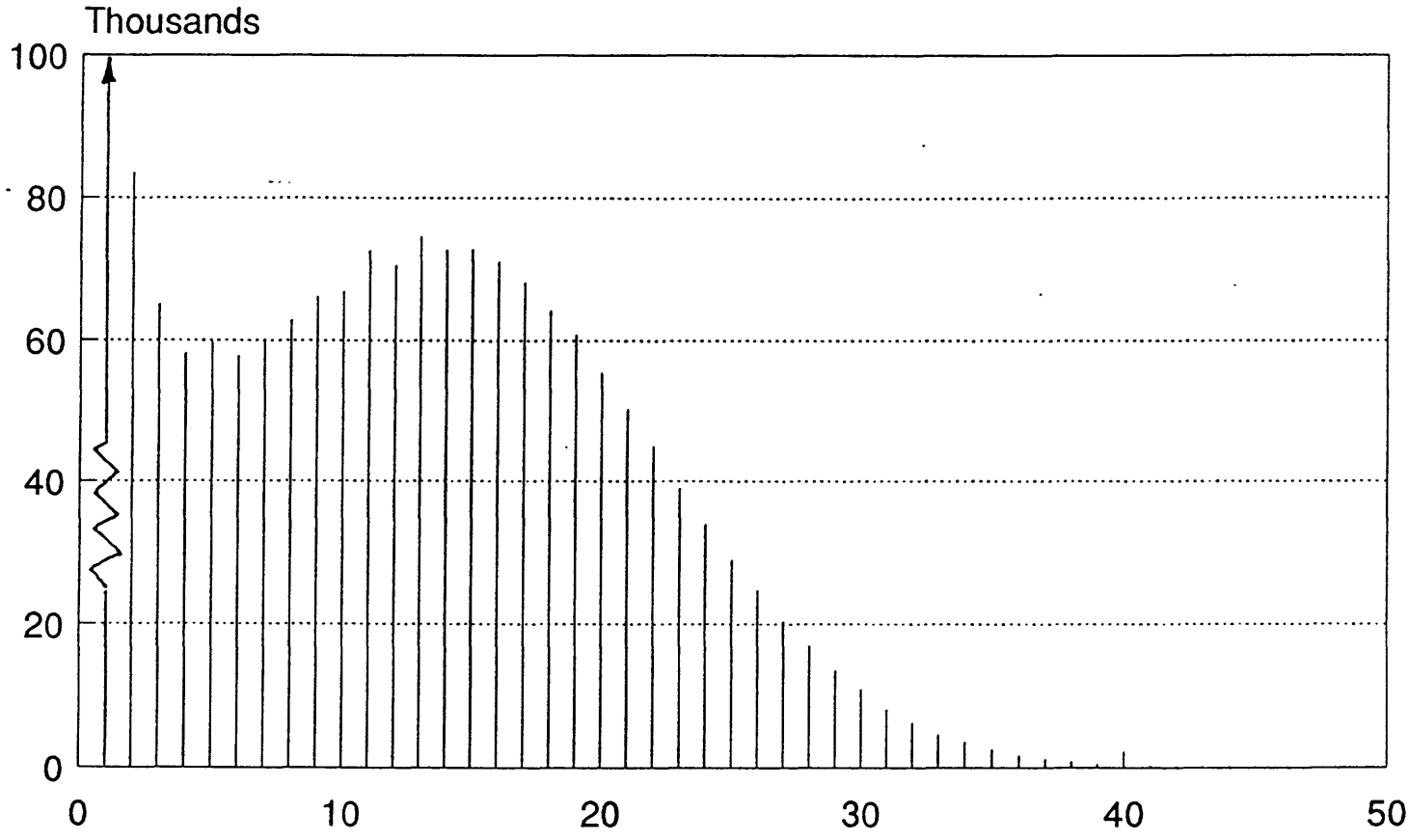

Fig. 6. Histogram of slope angle (degrees of arc) in the 1:100,000-scale San Jose quadrangle (maps 10 and 11). Bimodal distribution reflects vivid contrast between erosional and depositional topography (see also figs. 8 and 9)

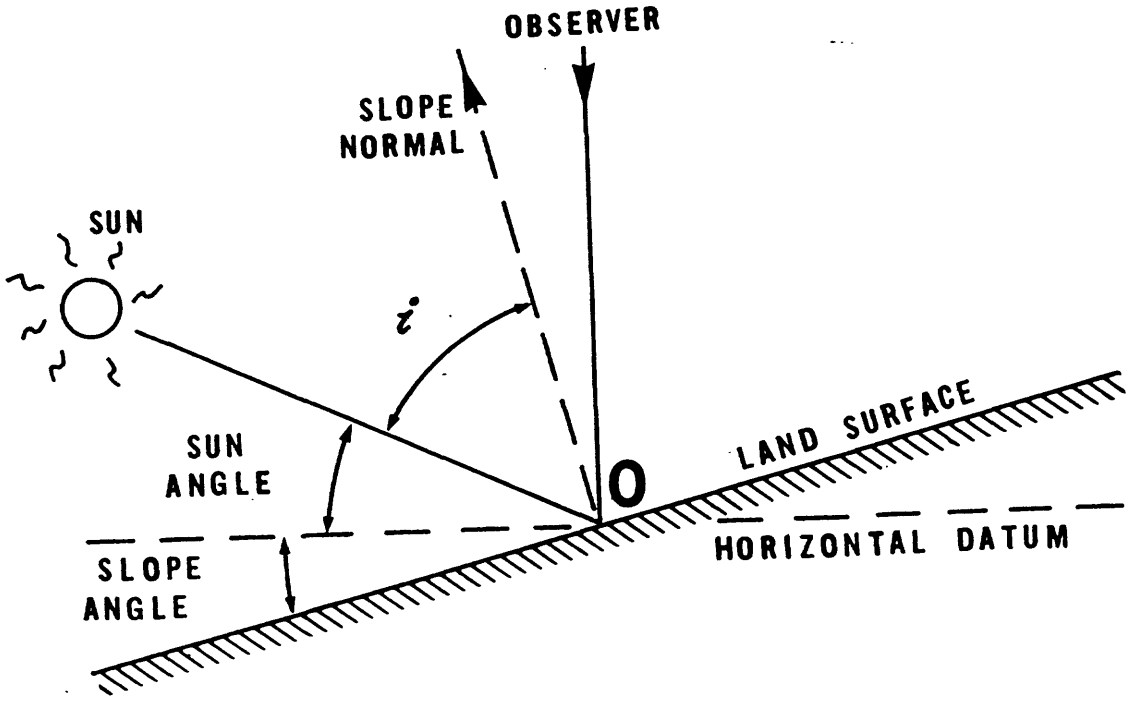

Fig. 7. Geometry for computing shaded relief (maps 13 and 14) from a DEM (after Batson and others, 1975). Point 0 is central elevation of the nine-point window used to calculate slope and aspect (see figure 2)

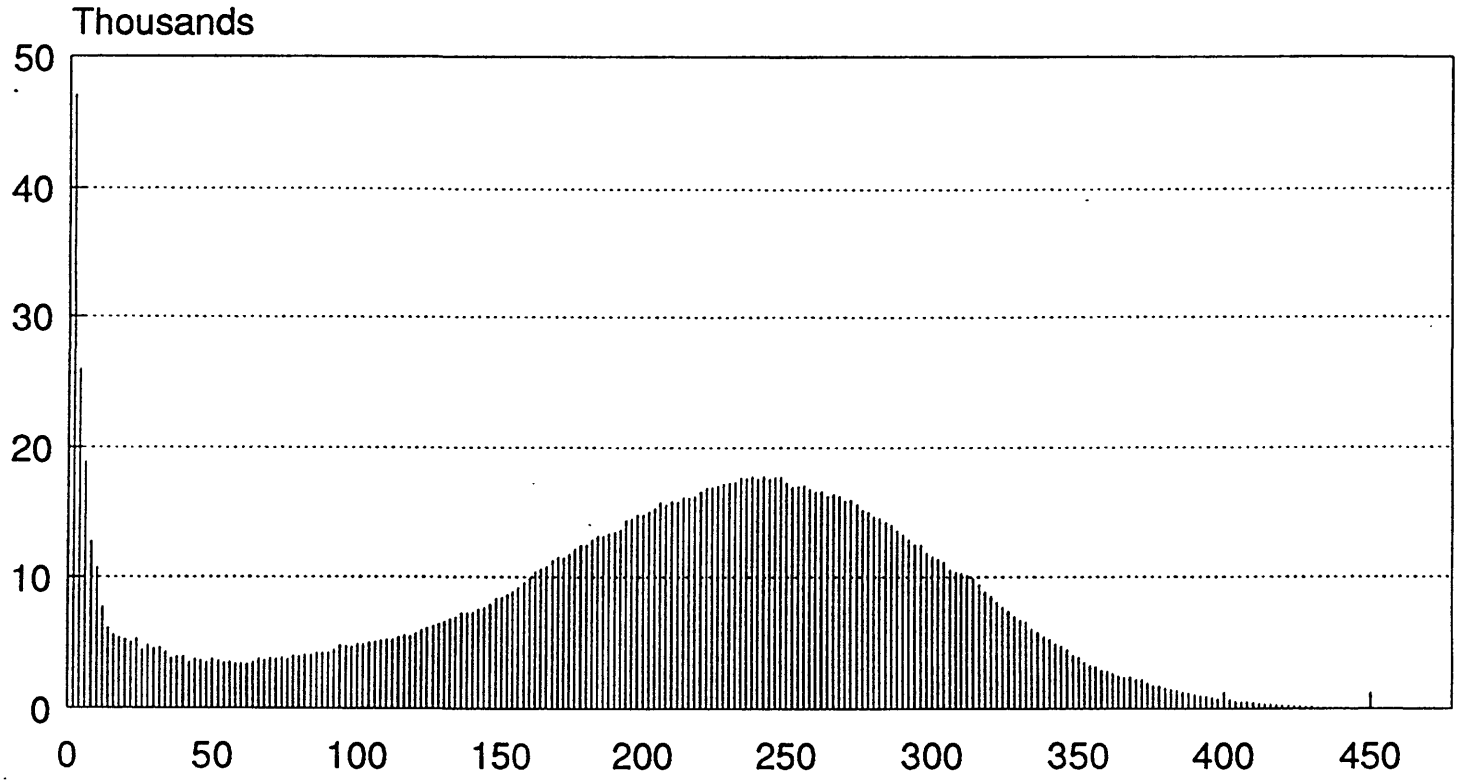

Fig. 8. Bimodal histogram of slope-reversal frequency (in number of slope reversals per km^2; see map 17) in the 1:100,000-scale San Jose quadrangle

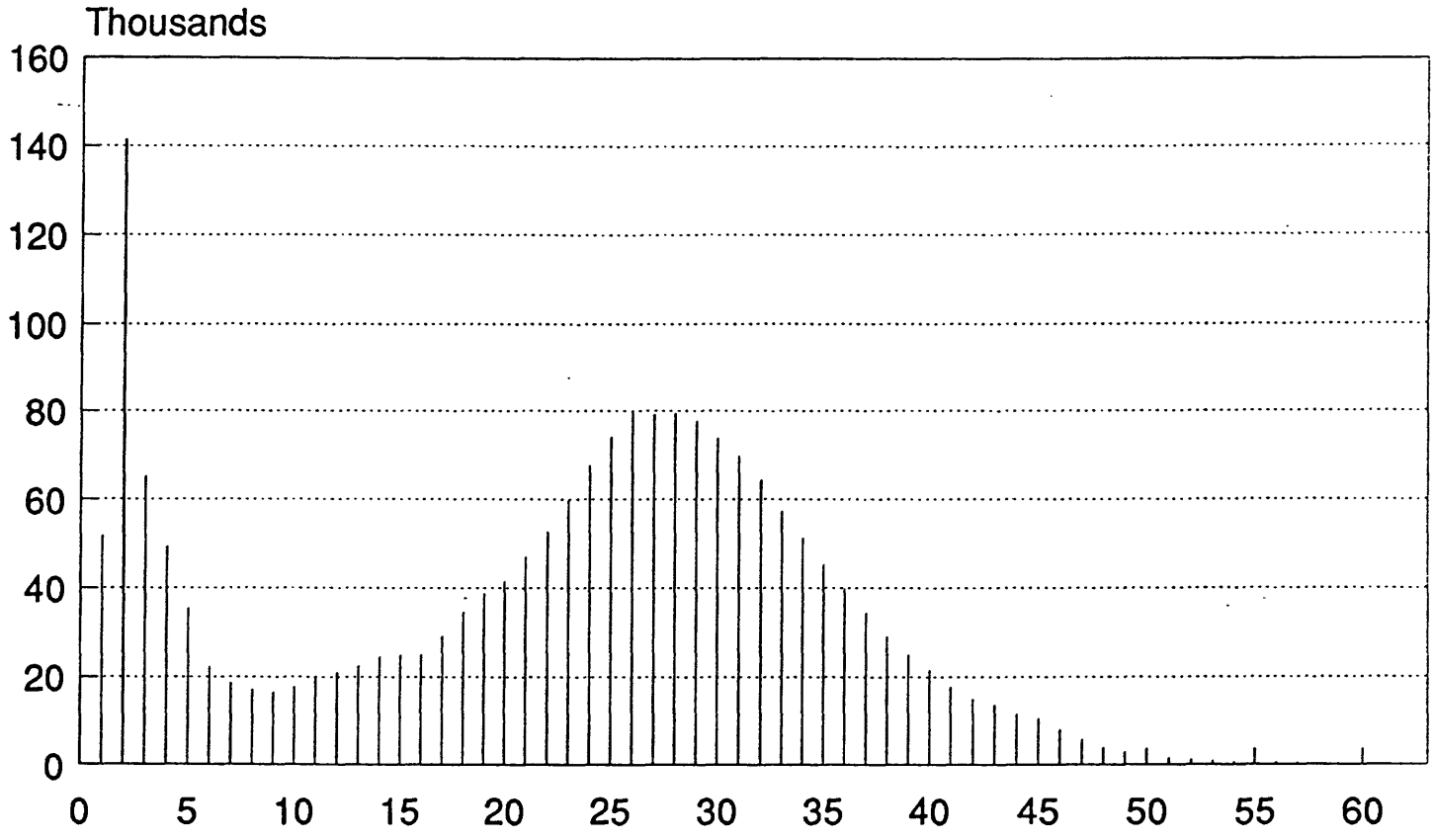

Fig. 9. Bimodal histogram of mean topographic curvature (in degrees of arc; see text for discussion and map 19) in the 1:100,000-scale San Jose quadrangle

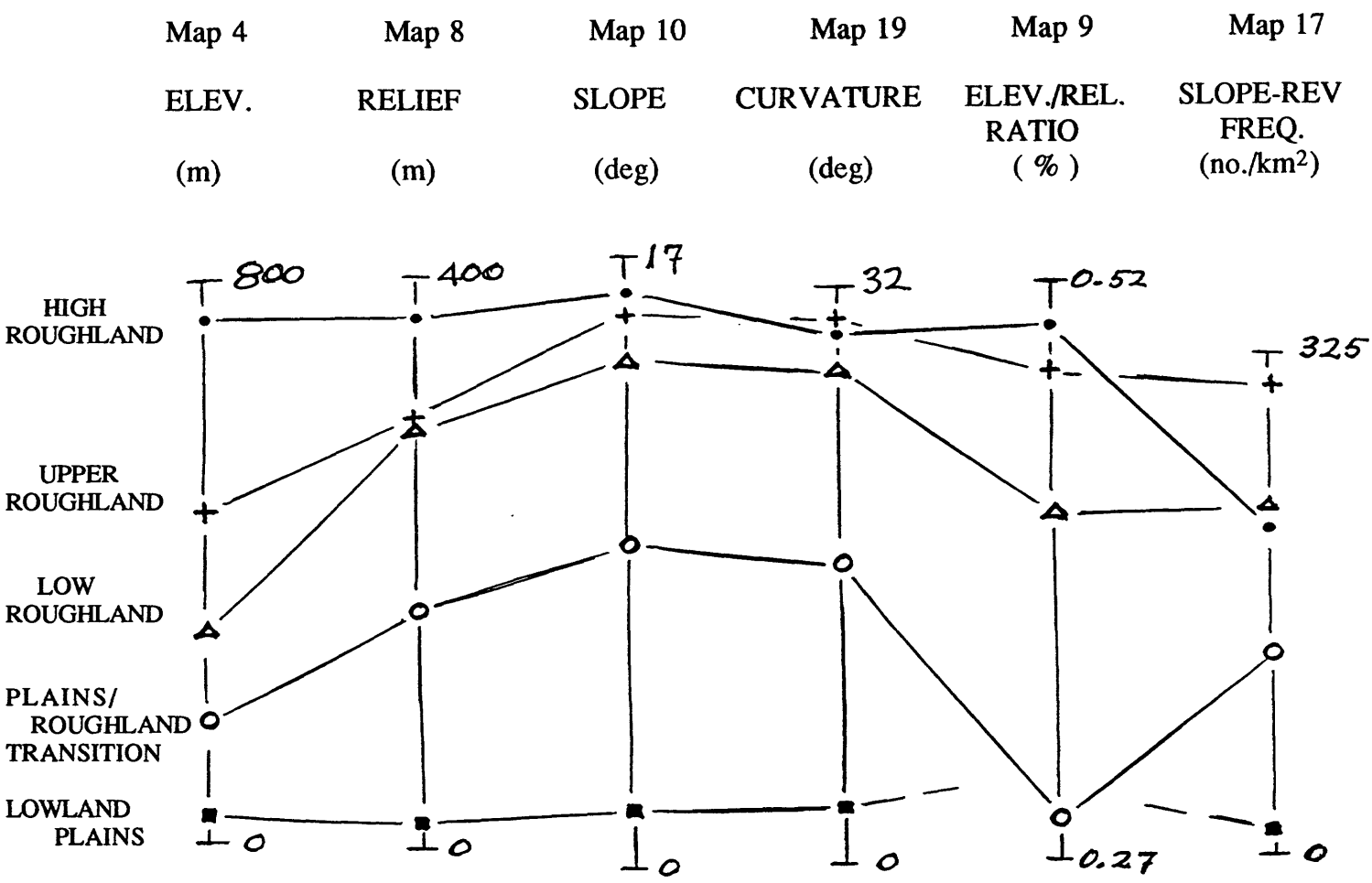

Fig. 10. Geometric signatures for five contrasting types of topography in the San Jose quadrangle (map 20). Signatures are averaged values (symbols) of six descriptive measures (six columns) at 253,011 locations in the quadrangle (corresponding maps: 4, 8, 10, 19, 9, and 17). Scales (for example, 0-800 m elevation) do not extend to full ranges of values observed for each measure. Values of elevation-relief ratio for plains are indeterminate

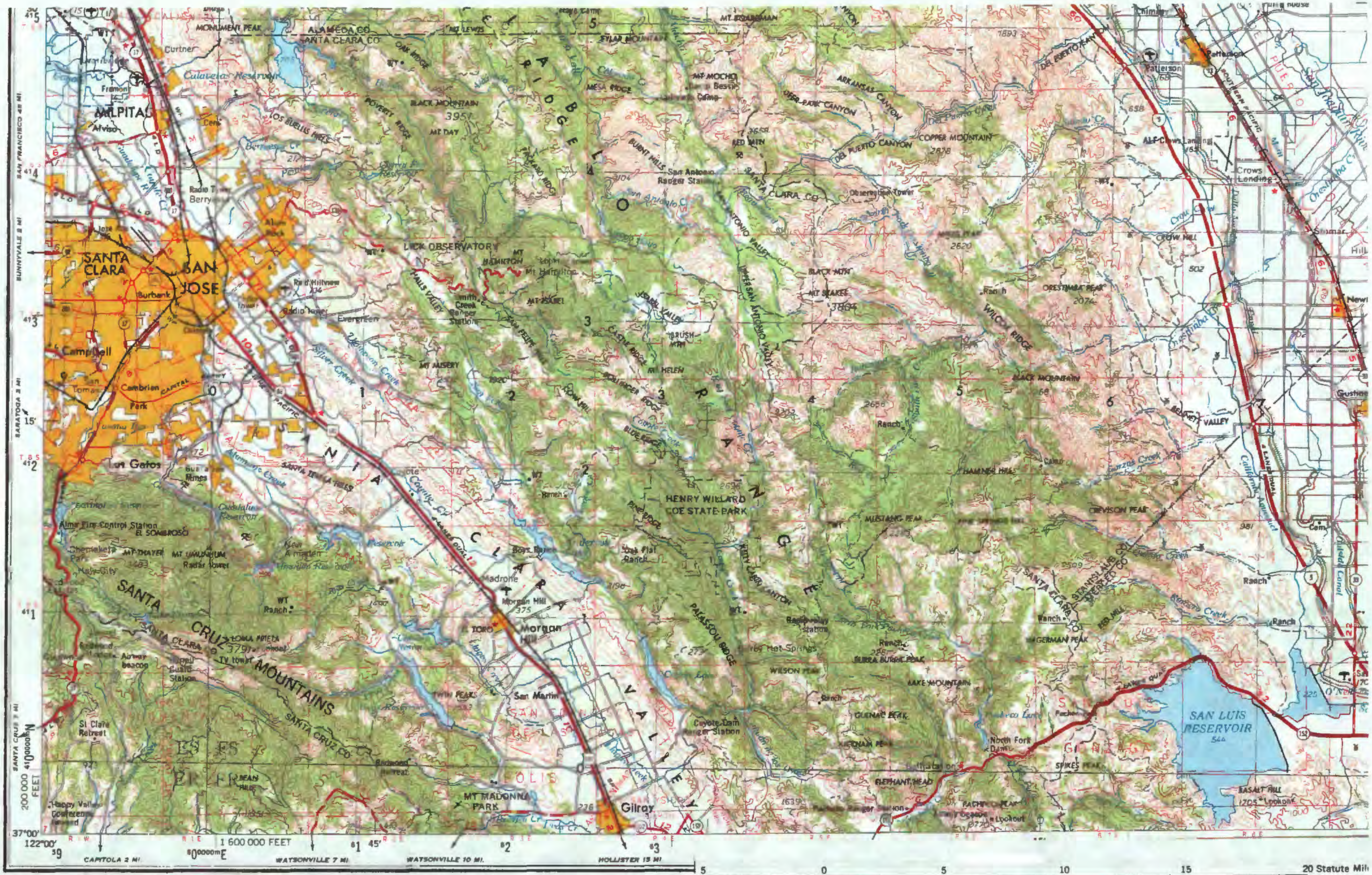

LOCATION MAP

2 GEOLOGY

EXPLANATION
(Selected Units; see Rogers, 1966)

- Qal — Alluvium
- Qf — Fan deposits
- Ep — Paleocene marine
- Ku — Upper Cretaceous marine
- KJf — Franciscan Assemblage
- ub — Mesozoic ultramafic intrusives

3 HYPSOGRAPHY

CONTOUR INTERVAL = 50 m
FROM 1:100,000 MAP

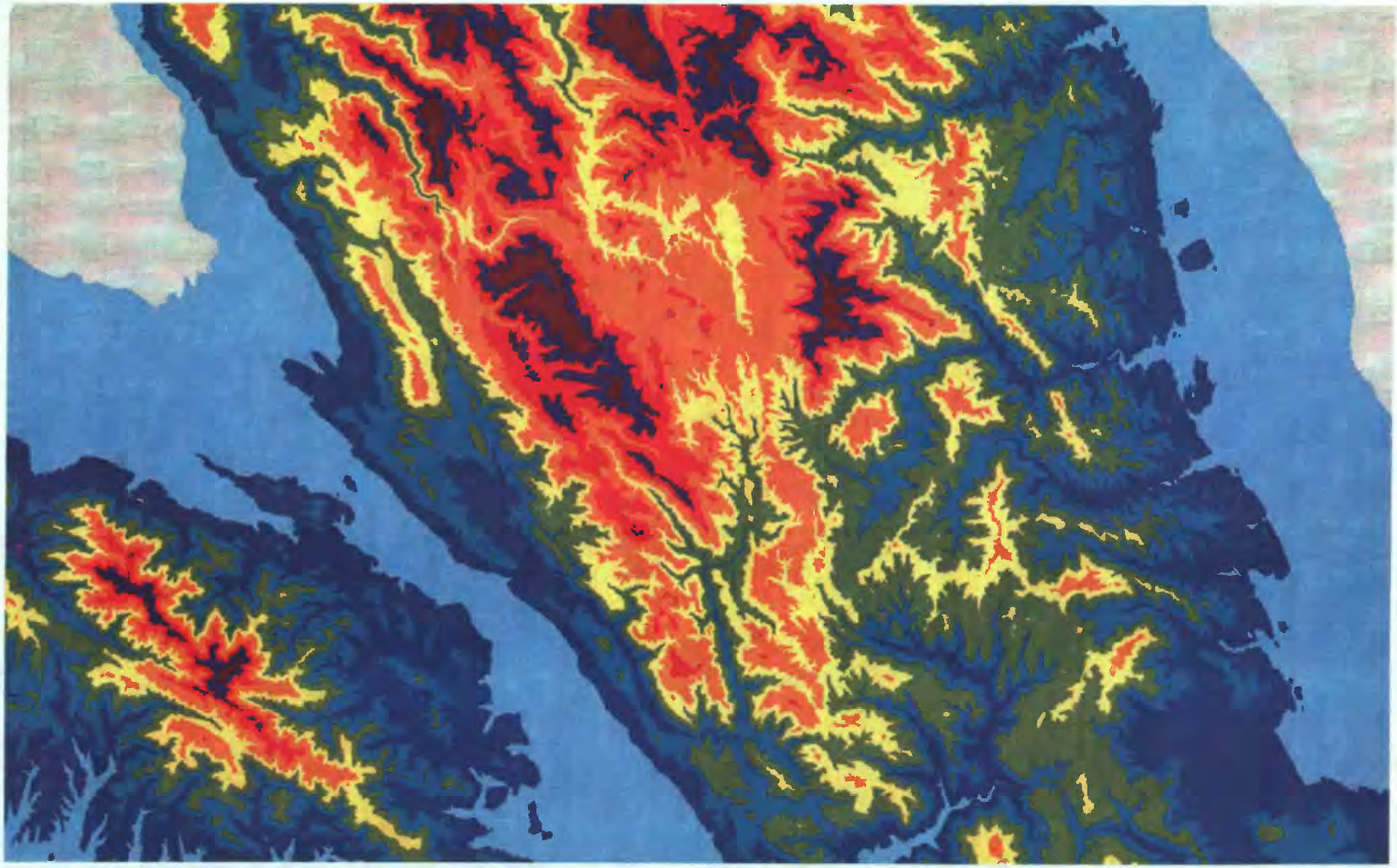

4 ELEVATION

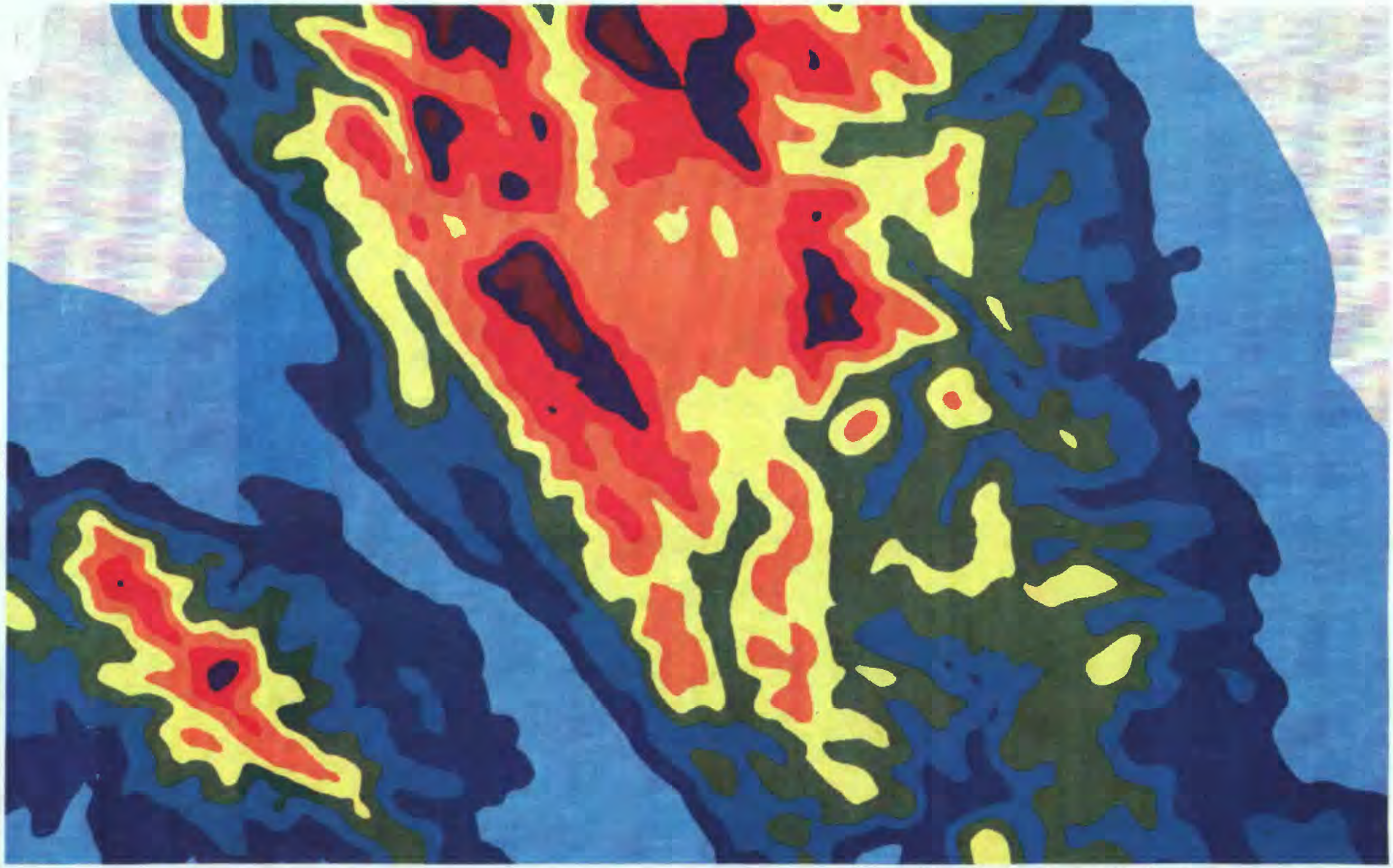

5 ELEV. MEAN

2 x 2 km units, CONTOURED

0m 26 128 256 385 513 641 770 898 1026 m

42-2

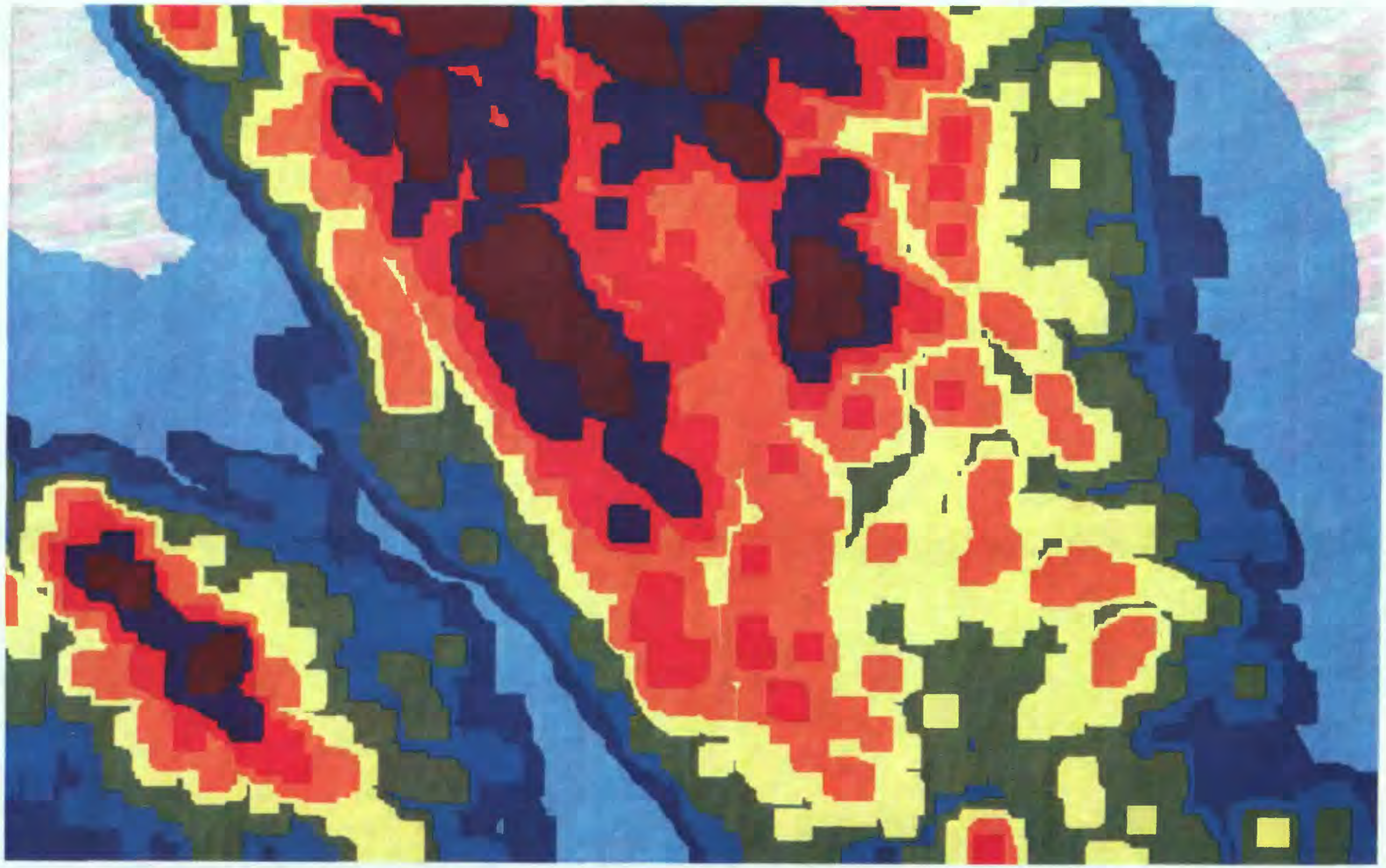

6 ELEV. MAX.

2 x 2 km window

0 26 128 256 385 513 641 770 898 1026 m

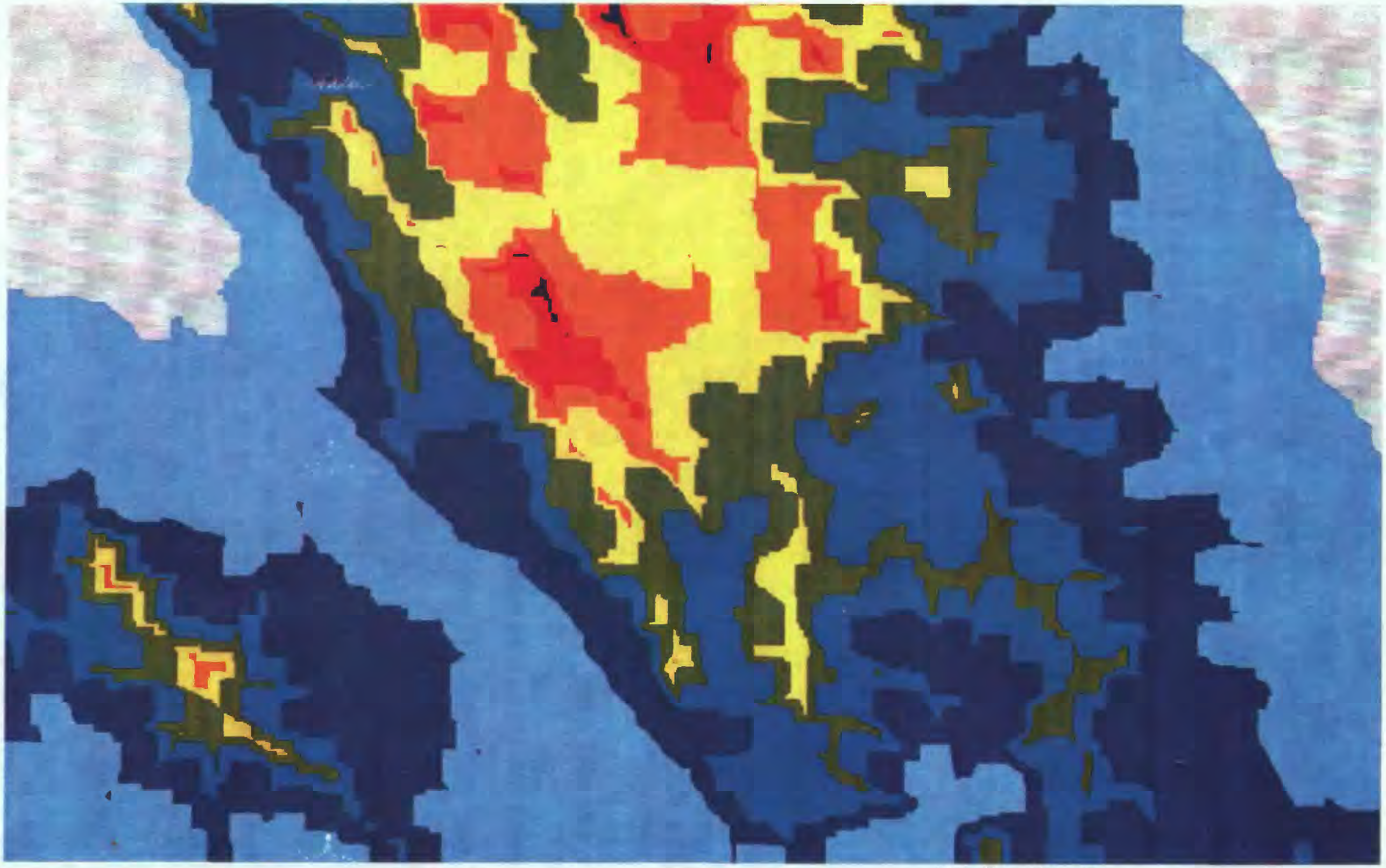

7 ELEV. MIN.

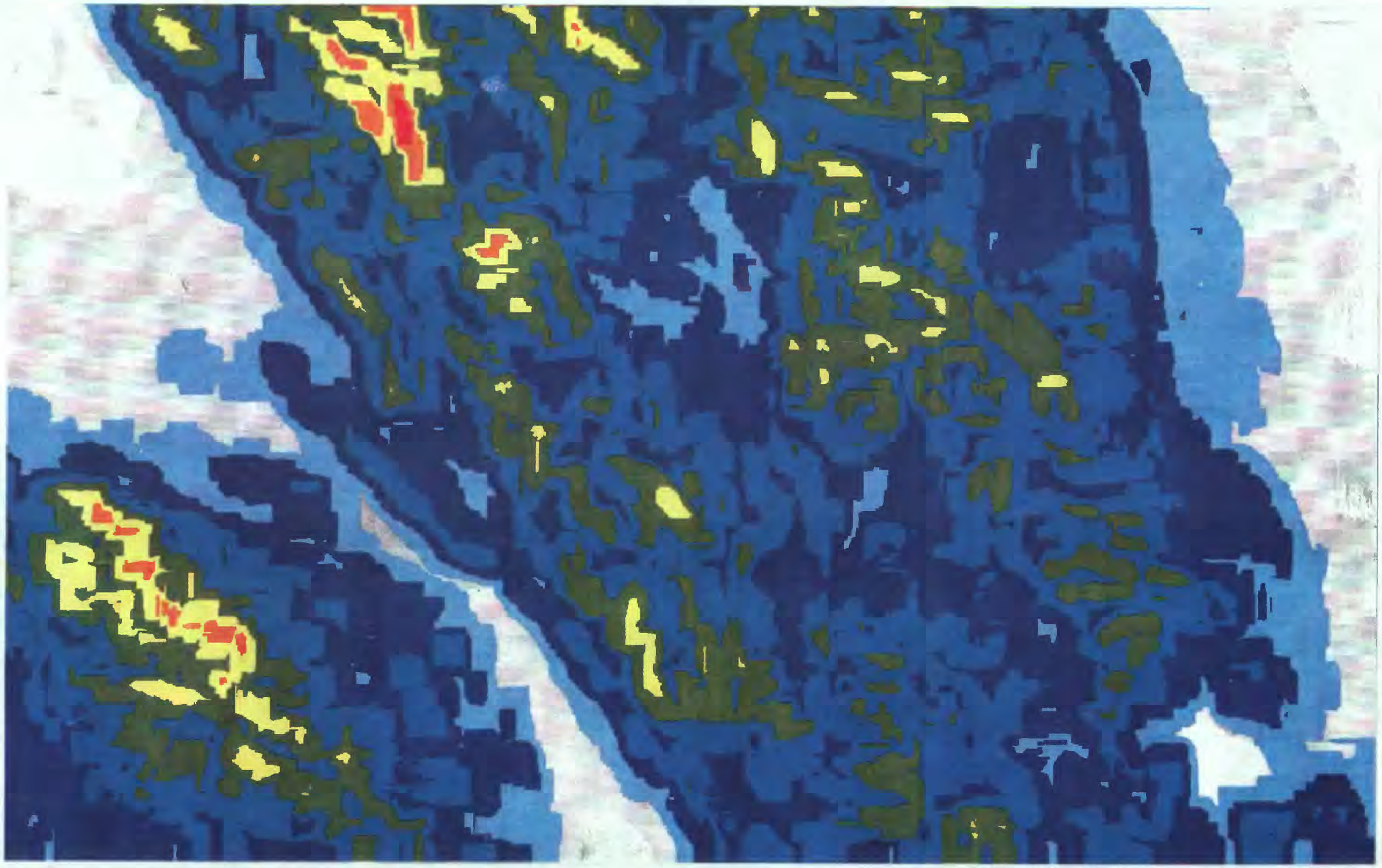

8 LOCAL RELIEF

DOES NOT APPLY IN LOW-RELIEF AREAS

DOES NOT APPLY IN LOW-RELIEF AREAS

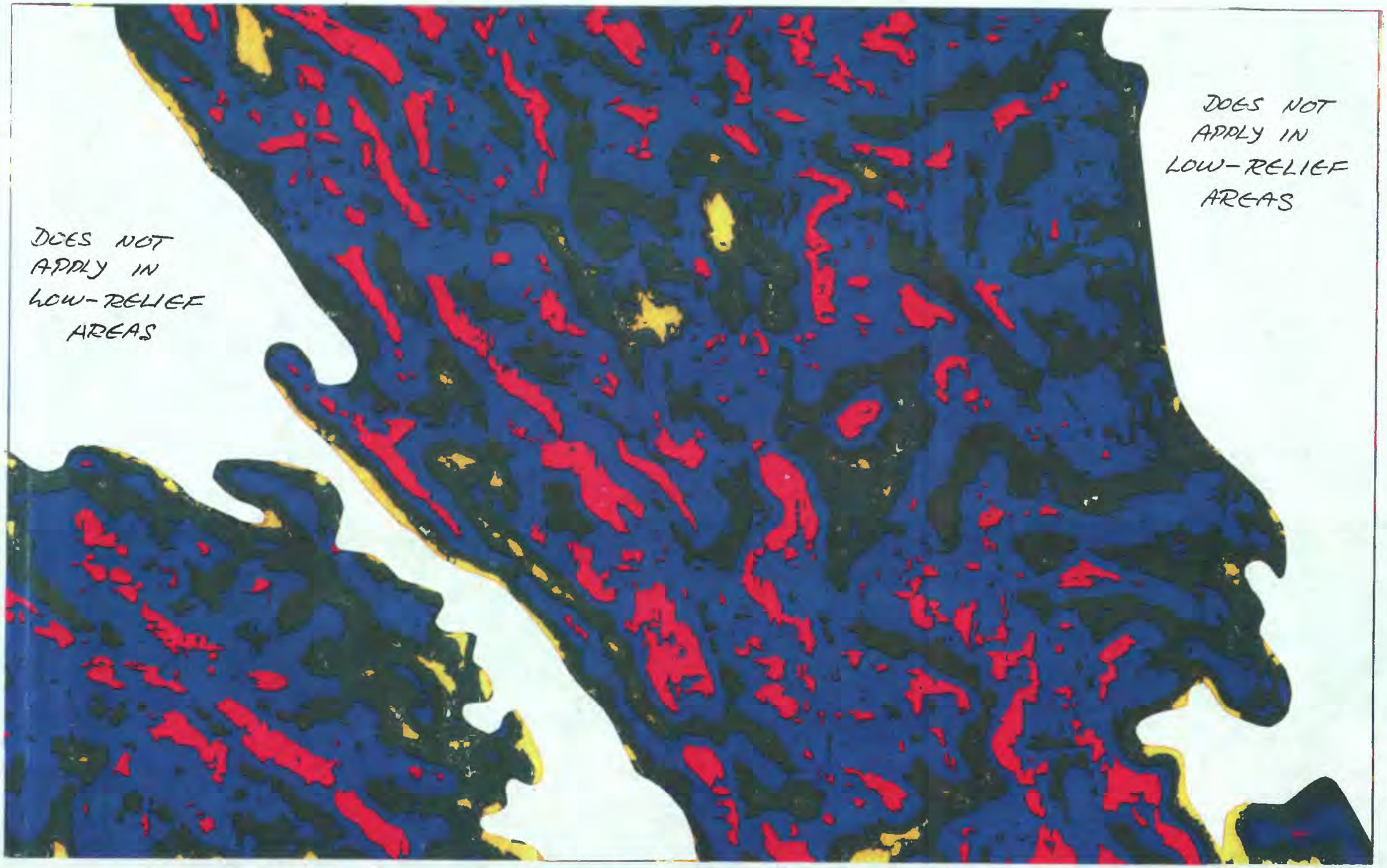

9 ELEV. RELIEF RATIO

$$\mathcal{E} = \frac{H_{mean} - H_{min}}{H_{max} - H_{min}}$$

0 .2 .4 .6 .8

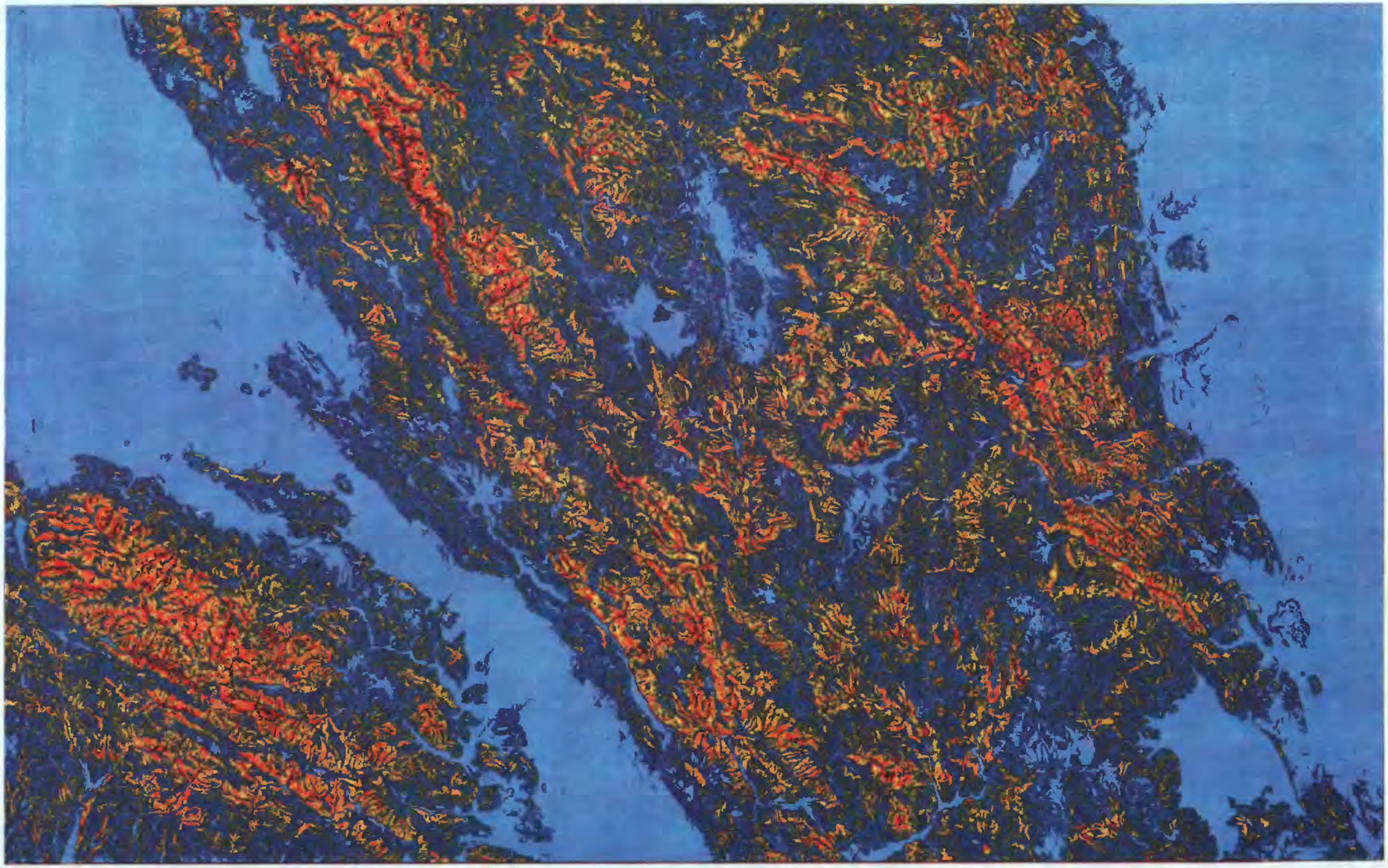

10 SLOPE ANGLE

on 3X3 pixel window

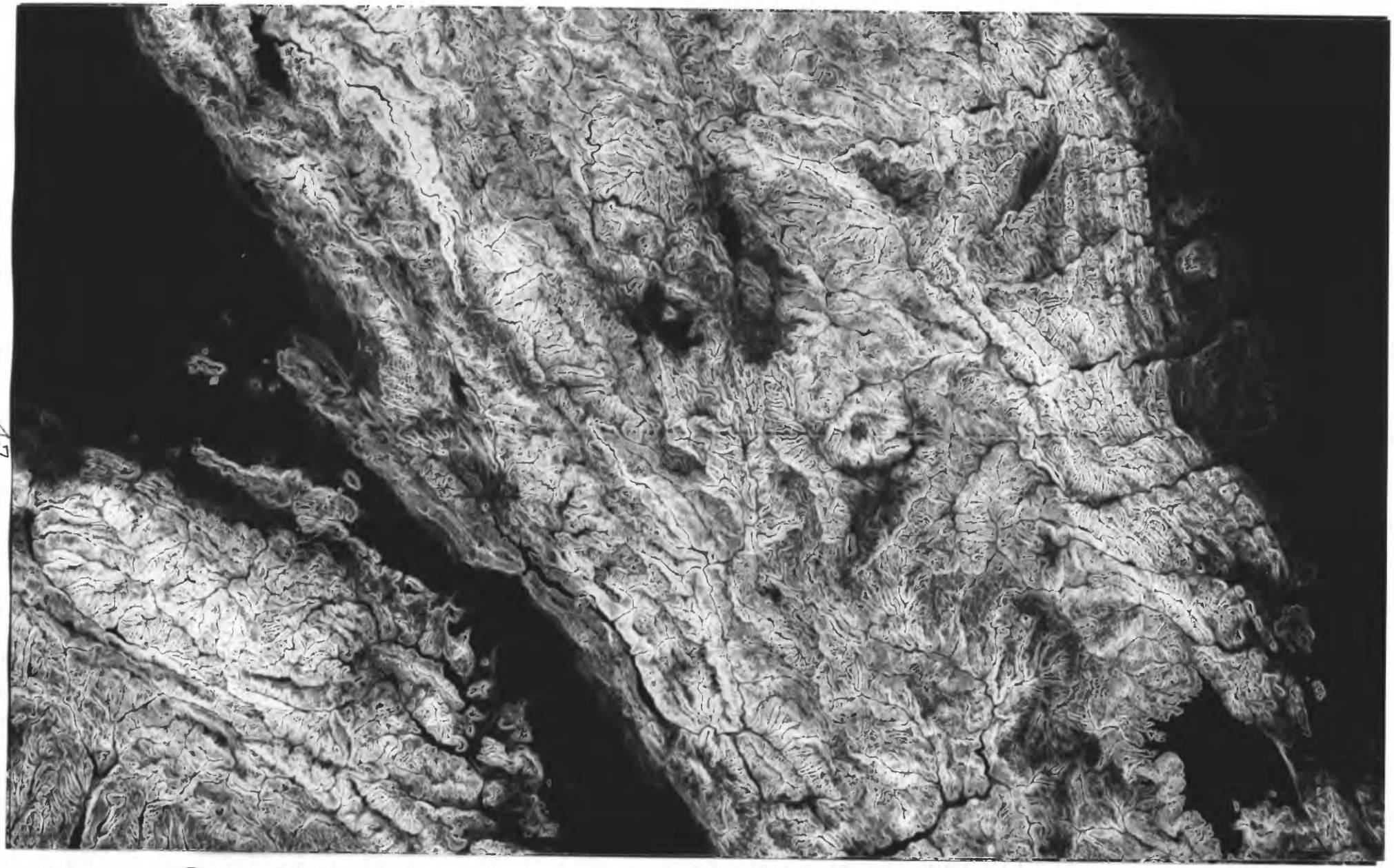

11 SLOPE

light ~ STEEP SLOPES
dark ~ low SLOPES

48

12 SLOPE ASPECT

black-to-white, clockwise

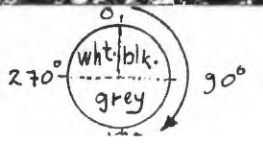

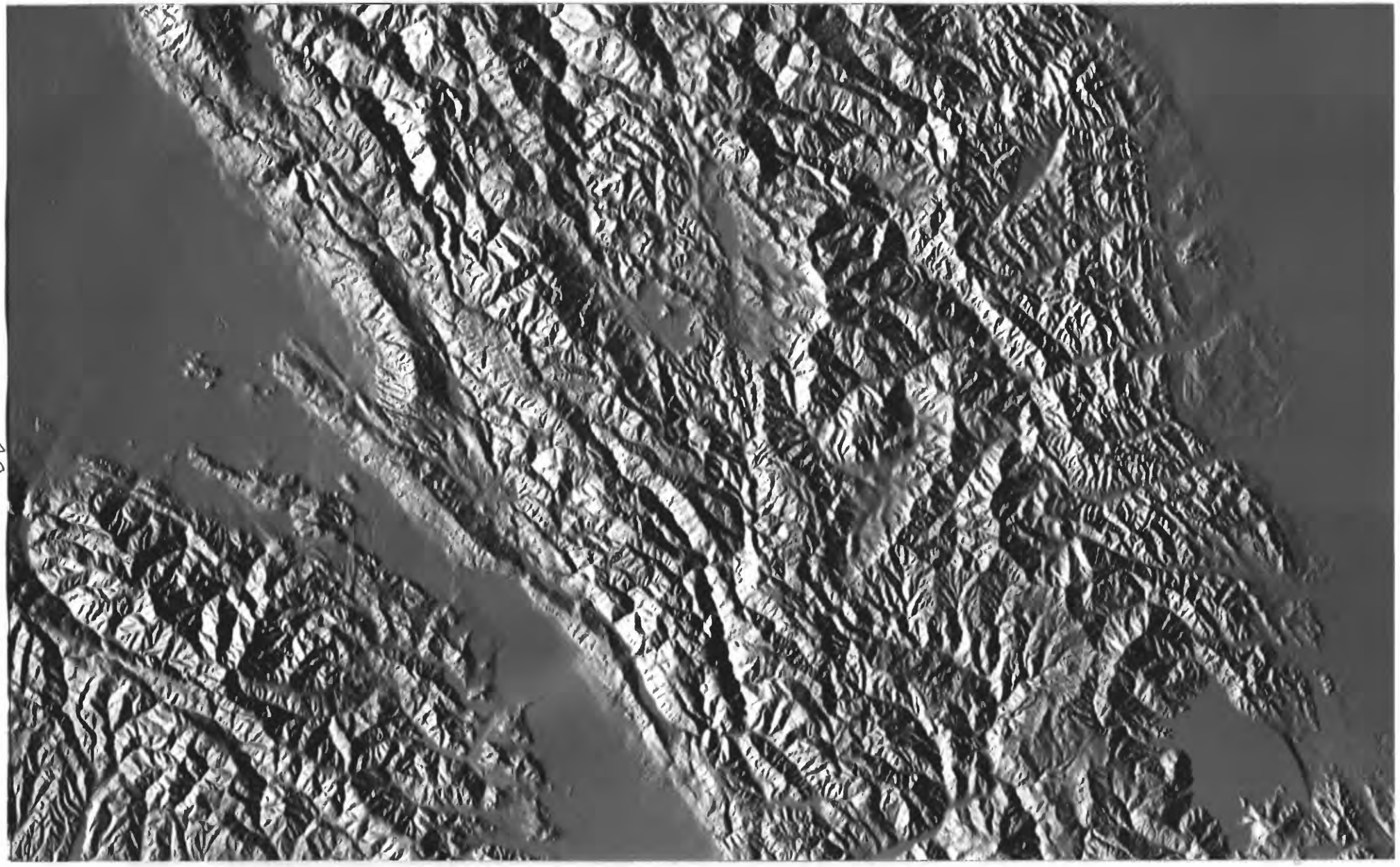

13 SHADED RELIEF W SUN DIRECTION

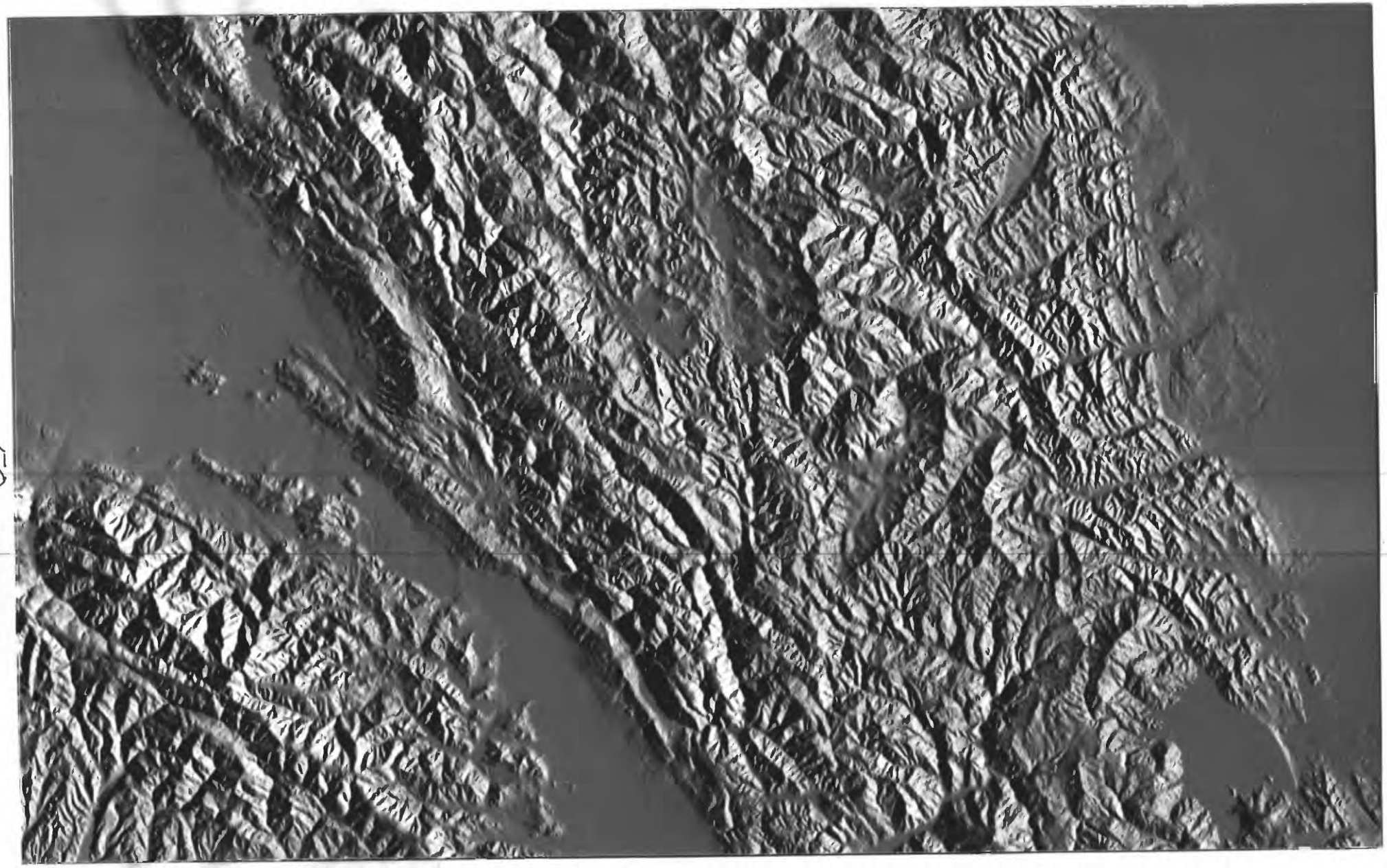

14 SHADED RELIEF E SUN DIRECTION

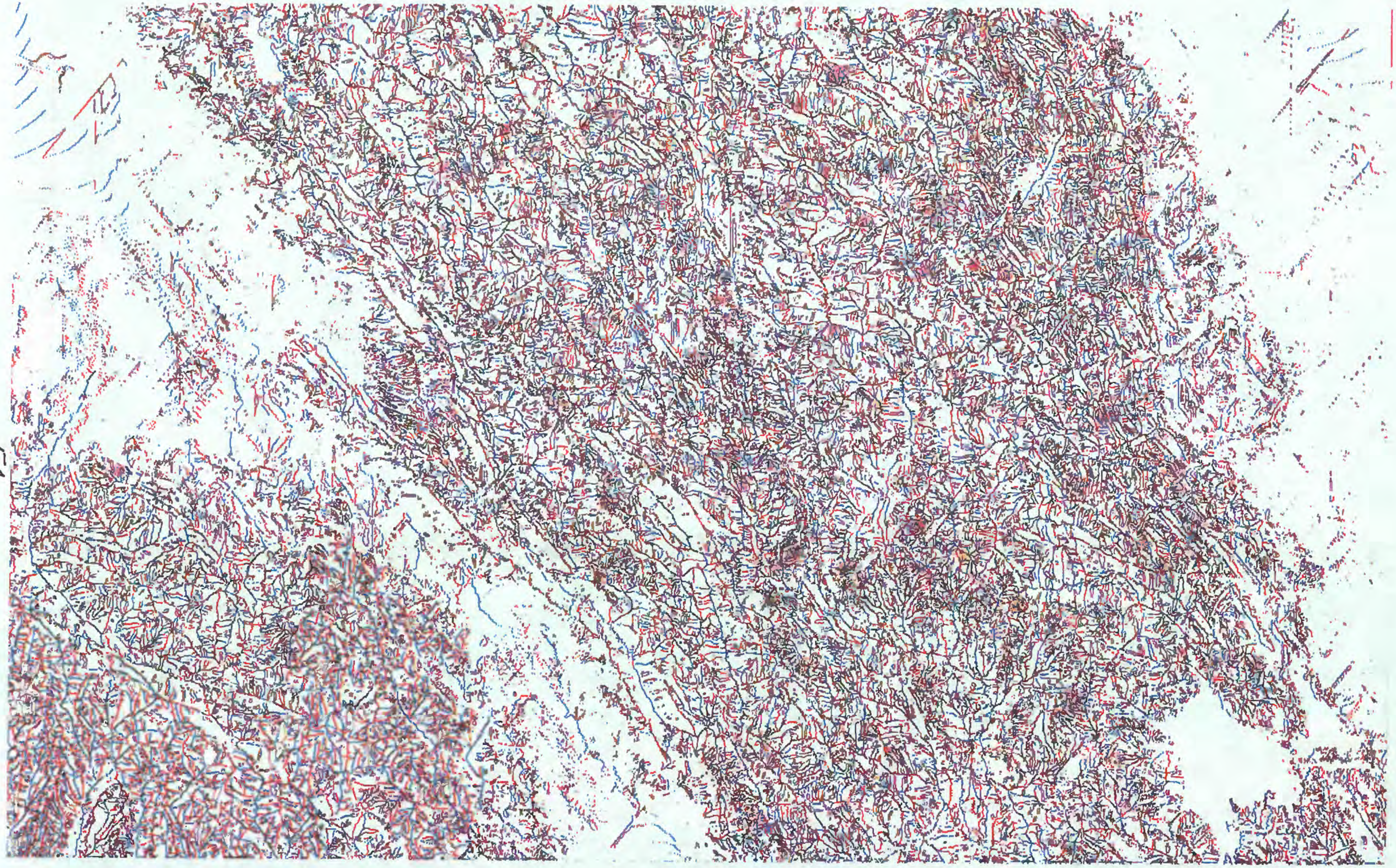

15 SLOPE REVERSAL (unfiltered)

~ – concave

~ – convex

52

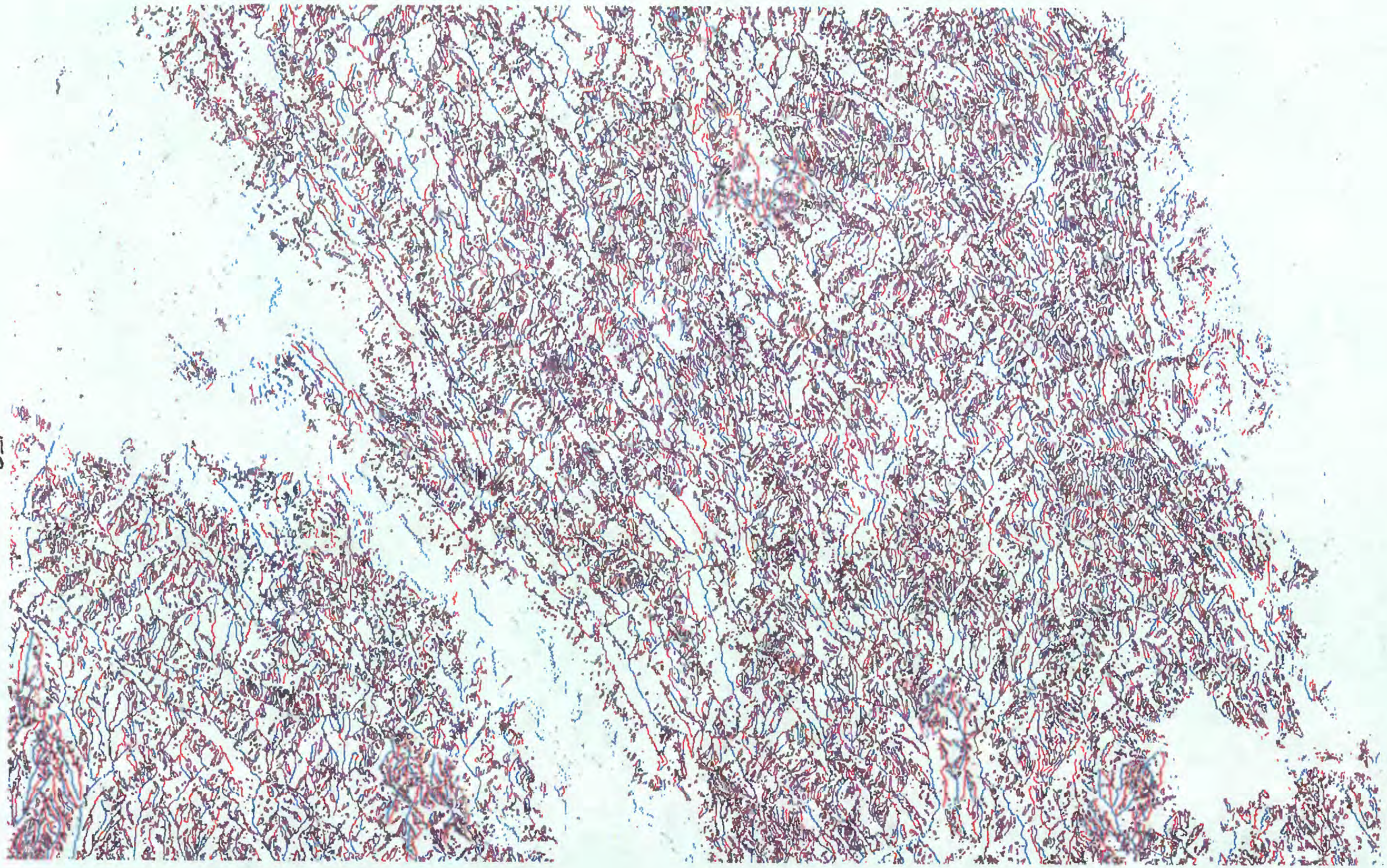

16 SLOPE REVERSAL (filtered)

– valleys

– ridges

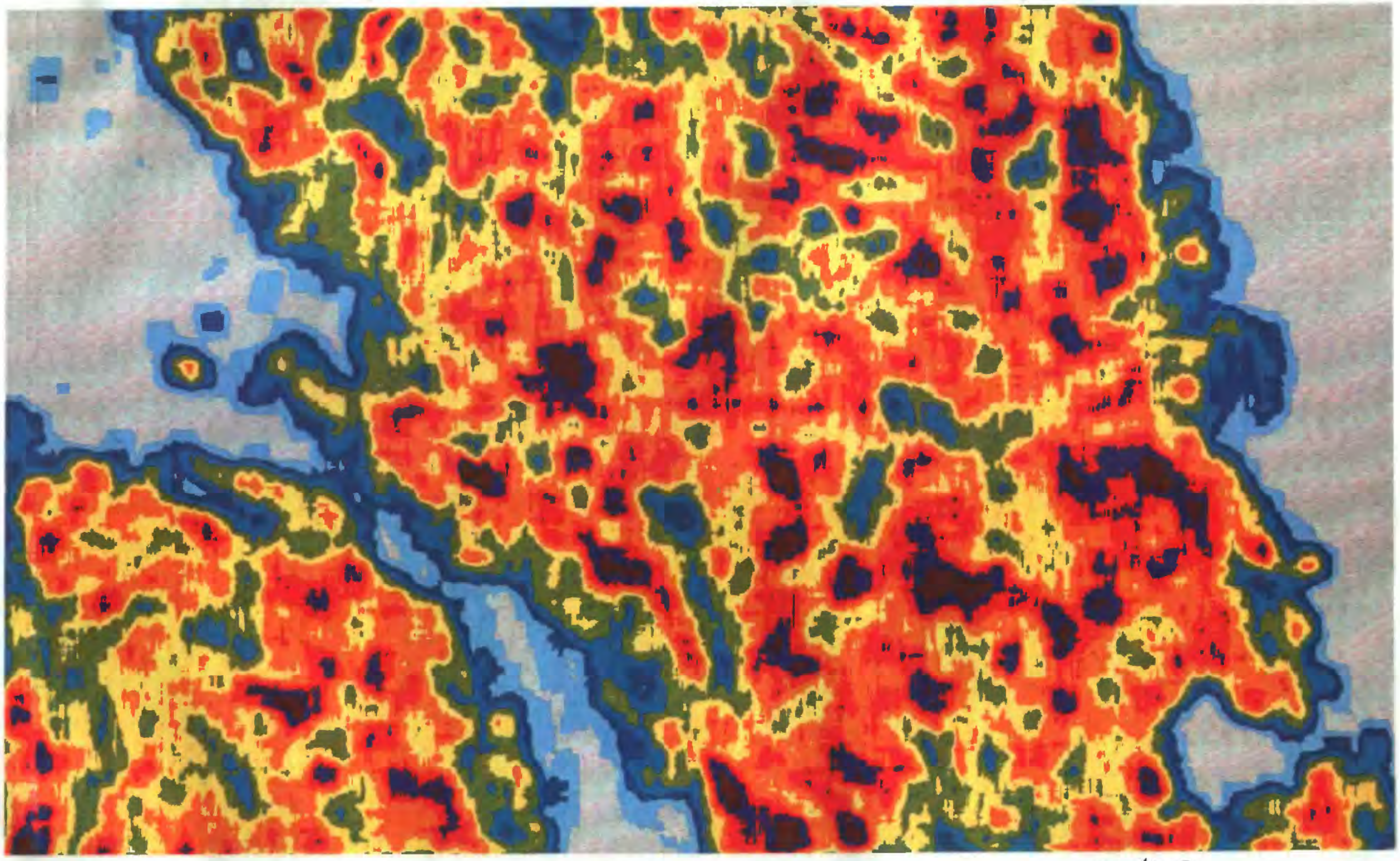

17 FREQ. SLOPE REVERSAL

0 96 192 288 384 478 no./km²

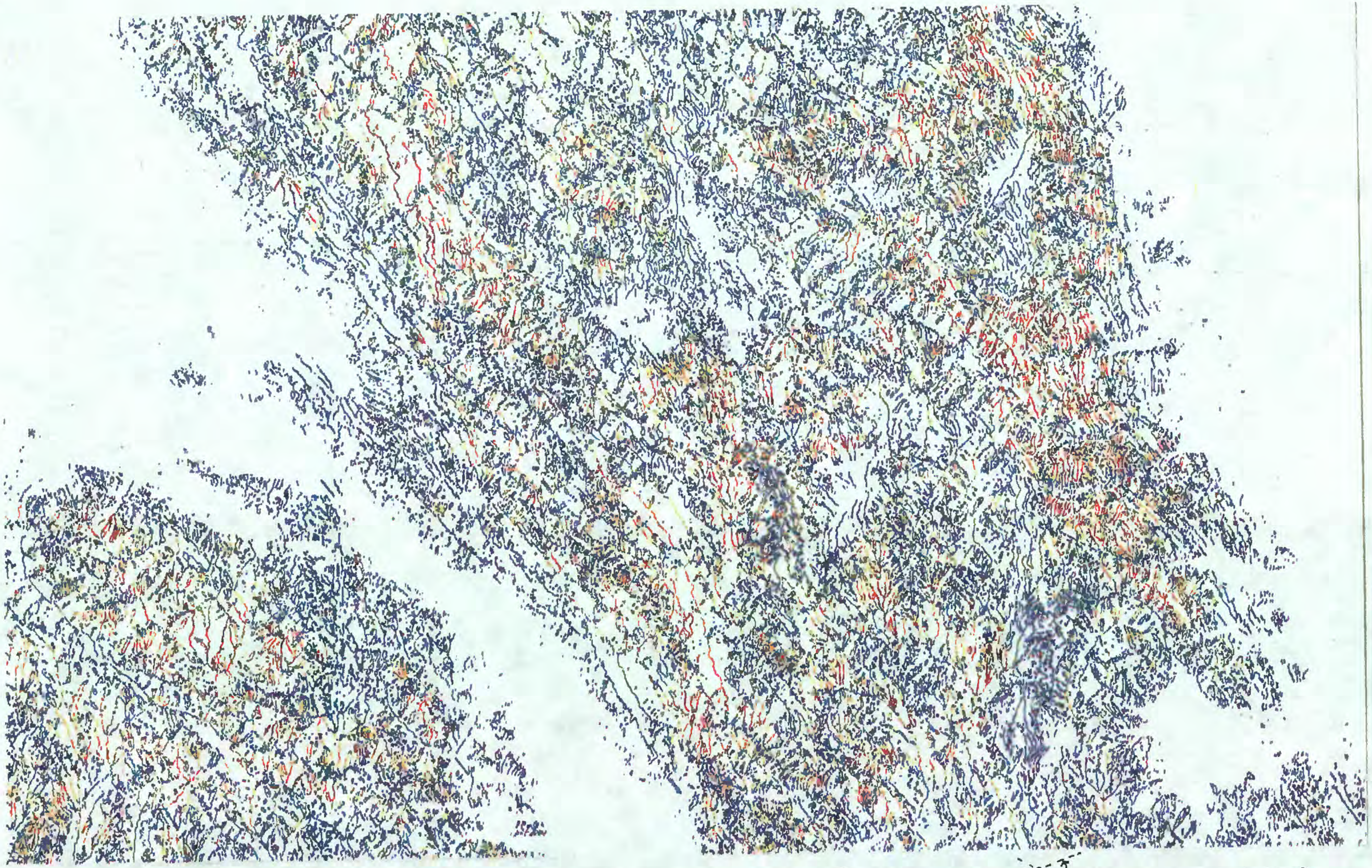

18 SLOPE CURV.

55

19

MEAN CURV.

on RIDGE TOPS & VALLEY BOTTOMS

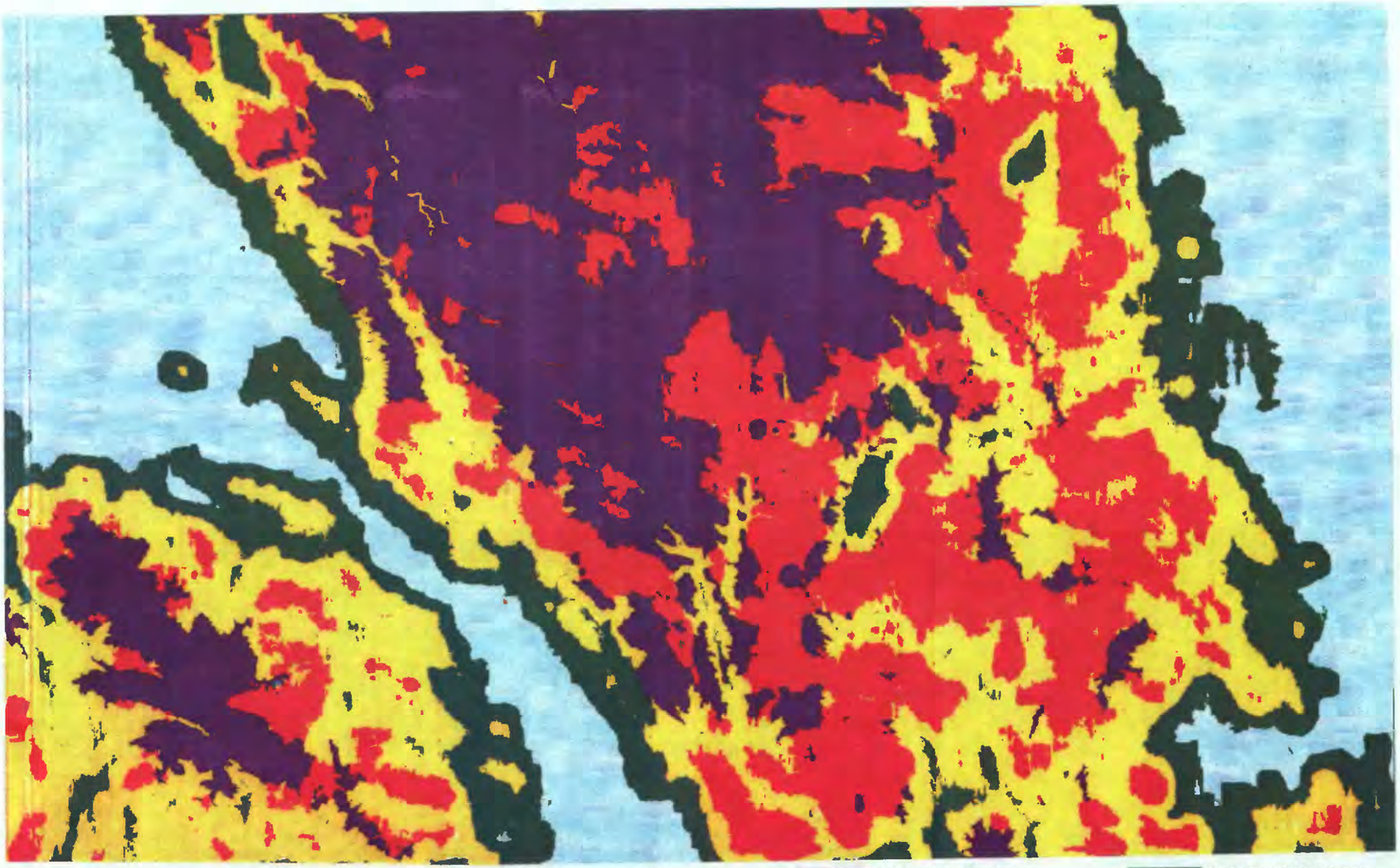

20 TOPO. TYPES

HIGH ROUGHLAND
UPPER ROUGHLAND
LOW ROUGHLAND

PLAINS/ROUGHLAND TRANSITION
LOWLAND PLAINS